Canadian Science Publishing

ARTICLE

Disentangling risks to an endangered fish: using a state-space life cycle model to separate natural mortality from anthropogenic losses

William E. Smith, Leo Polansky, and Matthew L. Nobriga

Abstract: State-space population models are becoming a common tool to guide natural resource management, because they address the statistical challenges arising from high observation error and process variation while improving inference by integrating multiple, disparate datasets. A hierarchical state-space life cycle model was developed, motivated by delta smelt (*Hypomesus transpacificus*), an estuarine fish experiencing simultaneous risks of entrainment mortality from out-of-basin water export and natural mortality. Notable model features included a covariate-dependent instantaneous rates formulation of survival, allowing estimation of multiple sources of mortality, and inclusion of relative observation bias parameters, allowing integration of differently scaled abundance indices and entrainment estimates. Simulation testing confirmed that two sources of mortality, process variation, and data integration parameters could be estimated. Delta smelt entrainment mortality was associated with environmental conditions used to manage entrainment, and recruitment and natural mortality were related to temperature, freshwater flow, food, and predators. Although entrainment mortality was reduced in recent years, ecosystem conditions did not appear to support robust spawning or over-summer survival of new recruits, manifesting as a 98% reduction of adults during 1995–2015.

Résumé : Les modèles démographiques d'espaces d'états sont des outils de plus en plus utilisés pour orienter la gestion des ressources naturelles parce qu'ils permettent de surmonter les difficultés statistiques découlant de grandes erreurs d'observation et d'une grande variabilité des processus, tout en améliorant l'inférence grâce à l'intégration de divers ensembles de données disparates. Un modèle hiérarchique d'espaces d'états du cycle biologique a été développé afin d'examiner l'éperlan à petite bouche (*Hypomesus transpacificus*), un poisson estuarien confronté à des risques simultanés de mortalité par l'entraînement associé à l'exportation d'eau vers l'extérieur du bassin versant et de mortalité naturelle. Parmi les éléments notables du modèle figurent la formulation de taux de survie instantanés dépendants de covariables, la possibilité d'estimer des sources de mortalité multiples et l'inclusion de paramètres associés aux biais d'observation relatifs, ce qui permet l'intégration d'indices d'abondance et d'estimations de l'entraînement de différentes échelles. Des essais de simulation ont confirmé que deux sources de mortalité, la variabilité des processus et les paramètres d'intégration de données peuvent être estimés. La mortalité par entraînement des éperlans à petite bouche est associée aux conditions ambiantes imposées pour gérer l'entraînement, et le recrutement et la mortalité naturelle sont reliés à la température, au débit sortant, à la nourriture et aux prédateurs. Bien que la mortalité par entraînement ait diminué au cours des dernières années, les conditions écosystémiques semblaient ne pas soutenir des frais robustes ou la survie estivale de nouvelles recrues, ce qui s'est traduit par une réduction de 98 % du nombre d'adultes durant l'intervalle de 1995 à 2015. [Traduit par la Rédaction]

Introduction

Human population growth and increasing use of natural resources has led to widespread ecosystem changes (Vitousek et al. 1997) and corresponding declines, or in some cases, endangerment of native fauna (McGill et al. 2015). The need to develop successful conservation and management strategies has driven advancements in quantitative modeling tools to inform complex decisions about allocation of natural resources and the biota that depend upon those resources. The statistical challenges are manifold when developing modeling tools for rare species. It can be difficult to sample rare species, resulting in observation error that may obscure the relationships between abundance and the environment and, therefore, the relative merits among resource management options (Harwood and Stokes 2003; Williams 2011). Populations at low densities may exhibit demographic stochasticity or process variation from multiple sources that must be disentangled from observation errors to make robust predictions about the consequences of conservation actions (Lande 1993). The management objective for population modeling is often to identify ways to balance recruitment, natural mortality, and anthropogenic mortality, requiring an understanding of how these vital rates interact to result in cumulative lifetime survival. Finally, declining population densities may necessitate new monitoring programs that must be integrated into existing population models over time, though new programs may be scaled differently with different catchabilities than older programs.

For natural populations that are shaped by both deterministic and stochastic processes and are often observed by multiple sampling programs, each with its own sources of error and bias, arguably the most robust approach to statistical population modeling is the state-space model, because it facilitates separation of the components of variability while allowing integration of a wide

Received 8 July 2020. Accepted 4 February 2021.

W.E. Smith, L. Polansky, and M.L. Nobriga. United States Fish and Wildlife Service, San Francisco Bay-Delta Office, Sacramento, California, USA.

Corresponding author: William Smith (emails: wes2316@gmail.com; william_e_smith@fws.gov).

Fig. 1. Map of the study area, created using ArcGIS ArcMap 10.6.1 and data provided by the US Geological Survey.

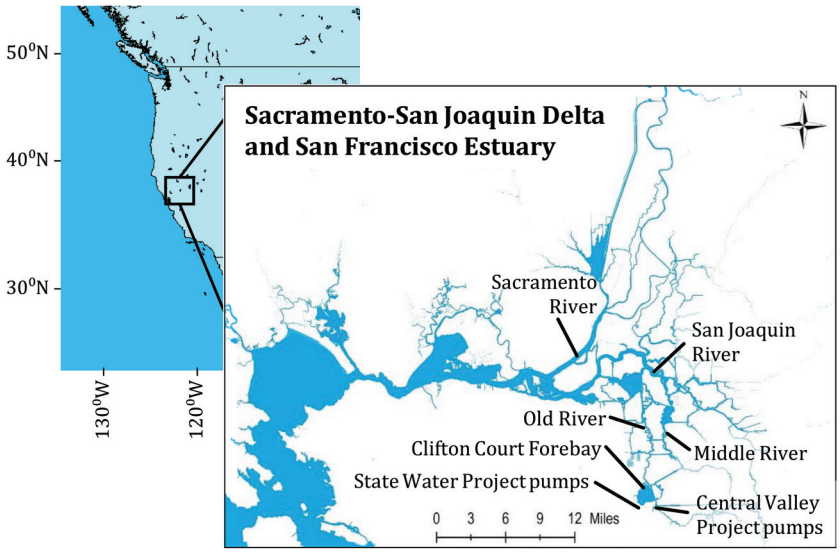

variety of information (Newman 1998; Meyer and Millar 1998). A (hierarchical) state-space modeling framework facilitates a probabilistic approach to population management and risk assessment by incorporating uncertainties in the values of parameters scaling the relative risks of mortality, the influence of temporal variation in ecosystem conditions on the population vital rates, and error in measurements of the population. State-space models have been applied to many types of populations, including insects (de Valpine and Rosenheim 2008), birds (Knape et al. 2013), and mammals (Servanty et al. 2010). In fisheries, state-space models have been used to simultaneously estimate per capita rates of fishing and natural mortality for many commercial fish stocks including common sole (*Solea solea*) (Rochette et al. 2013), Atlantic salmon (*Salmo salar*) (Massiot-Granier et al. 2014), northern cod (*Gadus morhua*) (Cadigan 2015), and yellowtail flounder (*Limanda ferruginea*) (Miller et al. 2016).

A principal concern when modeling fishery catch data and defining harvest limits is that parameters related to both fishing and natural mortality may not be estimable within the same model, though variation in both results in catch variation. For this reason, a common approach is to fix the natural mortality rate at an externally derived value and estimate the remaining losses as fishing mortality (Mangel et al.2013). Recent applications (Rochette et al. 2013; Massiot-Granier et al. 2014; Cadigan 2015; Miller et al. 2016) of state-space models demonstrate, however, that combinations of the number of deaths due to a source of mortality (e.g., fishery catch) and an index of abundance may be sufficient to extract information about both fishing and natural mortality rates. Importantly, Aanes et al. (2007) showed that process variation from two sources of mortality could be extracted from common catch-at-age and abundance data.

In most models of fished populations, fishery catch is known with little error, and fishing mortality may be estimated as a function of fishery effort (e.g., Rochette et al. 2013; Aanes et al. 2007). In other scenarios, another source of mortality and associated errors may be known, and covariates such as ecosystem conditions may drive the per-capita mortality process. Fishery models combine estimates of abundance with estimates of the number of deaths attributable to a particular source of mortality and associated errors, but mortality rates for any taxa could be estimated, like fishery catch, as a function of competing risks of mortality.

Here, we describe a state-space population model motivated by the population processes of an endangered fish, delta smelt (*Hypomesus transpacificus*), that is subject to entrainment in large water diversions. This model includes recruitment and life stage-specific survival to separate sources of mortality, predict per-capita rates of mortality as a function of management quantities, and test hypotheses about factors influencing vital rates. Model performance is first evaluated by fitting models to simulated datasets and assessing estimability of model parameters. Guided by the findings from the simulation study, the model is then used to assess the population status of delta smelt and is applied to evaluate management strategies and test hypotheses about the associations between vital population rates, ecosystem conditions, and regulations to limit water diversions.

Case study: the decline of California's delta smelt

Delta smelt is an endangered osmerid fish, endemic to the San Francisco Estuary in California, USA. The delta smelt exists at the nexus of high-stakes natural resource management, high observation error, and critical population status (Moyle et al. 2018). Delta smelt may once have been one of the most common fish in the upper portion of the San Francisco Estuary, the Sacramento–San Joaquin Delta (hereinafter, Delta), but have declined to near extirpation in recent decades. Major changes to the physical structure of the Delta since the California Gold Rush, a series of biological invasions beginning in the latter 19th century (Nobriga and Smith 2020), and increasingly greater fractions of fresh water captured in storage or diverted (Cloern and Jassby 2012) may have each contributed to the decline of delta smelt. Delta smelt were listed as threatened under the US and State of California Endangered Species Acts in 1993 and as endangered under the California Endangered Species Act in 2009 (Moyle et al. 2018). Entrainment of delta smelt in large water diversions since the completion of the Central Valley Project in 1951 and the State Water Project in 1968 has received special attention as a factor contributing to their decline (Brown et al. 2009; Moyle et al. 2018).

The Delta forms at the confluence of the Sacramento and San Joaquin rivers (Fig. 1). The physical structure of the Delta has been considerably altered from its natural state for flood control and agriculture, resulting in isolation from adjacent floodplains (Whipple et al. 2012; Andrews et al. 2017), reduction in suspended sediments and system productivity, and cumulative changes to the duration, magnitude, and timing of inflowing fresh water (Cloern and Jassby 2012). The Delta is the primary transfer point for the large-scale redistribution of surface water from northern to central and southern California. The southern portion of the Delta,

including the San Joaquin, Old, and Middle rivers (the South Delta; Fig. 1), conveys water to two of the largest water diversions in the world, the Tracy and Banks pumping plants, located on the Old River. These pumping plants are part of the US government's Central Valley Project (CVP) and California's State Water Project (SWP), respectively. Although tidal action plays a major role in hydrodynamics in the Delta's numerous channels (Andrews et al. 2017), the combined water diversions from Tracy and Banks pumping plants are often sufficient to reverse the net flow direction of Old and Middle rivers, causing water to flow upstream. This phenomenon draws Sacramento River water across the Delta to the pumping plants and can cause the entrainment of fish (Kimmerer and Nobriga 2008). Collectively, the projects exported as much as 8.5 billion m^3 of Sacramento–San Joaquin Delta water per year between 1995 and 2014 (ftp://ftp.dfg.ca.gov).

As entrainment of delta smelt is mitigated at the cost of water to supply tens of millions of people in southern California with drinking water and a multibillion dollar agricultural industry (Grimaldo et al. 2009; Moyle et al. 2018), the stakes in the water management strategy described above are high. Management of delta smelt entrainment has been a topic of contentious scientific debate (Kimmerer 2011; Miller 2011) and litigation (2010 US District Court ruling, OCAP Case 1:09-cv-00407-OWW-DLB). Efficient management of natural resources requires periodic assessment of past actions and evaluation of the effectiveness of regulatory criteria, such as limits on the export of water. Population models are useful quantitative tools for assessing effects of past conservation actions, evaluating the quality of management criteria, and comparing actions to manage populations in the future.

Delta smelt mortality risks can be divided into the risk of entrainment and the risk of mortality from all other sources. While many sophisticated models have been applied to delta smelt, none have sought to quantify per-capita entrainment risk as a function of the variables used to manage delta smelt entrainment, focusing instead on identification of the factors with the greatest influence on recruitment and survival (Maunder and Deriso 2011; Miller et al. 2012; Kimmerer and Rose 2018; Polansky et al. 2021). With newly available estimates of the number of entrained fish and, critically, the associated observation errors (Smith et al. 2020; Smith 2019), an opportunity to draw inference from population models that disentangle the relative contributions of different mortality sources to survival, and extend this understanding to population growth rate consequences, has emerged.

The life cycle model here integrates abundance indices (Polansky et al. 2019) with entrainment and associated errors (Smith et al. 2020; Smith 2019) into a single population model using a state-space model framework to quantify entrainment mortality as a function of existing management quantities and does so within the context of time-varying natural mortality rates (i.e., the survival models are functions of both natural and entrainment processes). Three management hypotheses are tested: (*i*) entrainment mortality is related to Old and Middle river flow, (*ii*) entrainment mortality at a given level of Old and Middle river flow depends on water clarity, and (*iii*) the management regime beginning in 2007 was associated with significantly lower delta smelt entrainment mortality. The model is then used to predict future mortality and population growth given alternative ecosystem and water operations conditions.

Materials and methods

Data

Data to fit the model consisted of time series of population abundance indices (Polansky et al. 2019), entrainment estimates of postlarvae (Smith et al. 2020) and adults (Smith 2019), and a collection of salient vital rate covariates used to predict recruitment, natural mortality, and entrainment mortality (Tables 1 and 2). A cohort year was defined by the birth of a cohort, beginning in March. Delta smelt is an annual fish, so a cohort year ended the following April after the spawning season. For example, cohort 1995 was first observed as early postlarvae in May of calendar year 1995 and finally as final spawn or postspawn adults in April of calendar year 1996. Here we focus on birth cohort years 1995–2015 and partition the species into seven life stages: early (May) and late (June) postlarvae, juveniles (July–August), early (October–November) and late (January–February) subadults, and early (March) and late (April) adults (Table 1). Although life stages represented a temporal scale of 1–3 months, water operations for delta smelt conservation are actively managed at a subweekly scale, so the life cycle model was a coarse abstraction of the delta smelt population and conservation schedule.

The abundance indices used here incorporated length-based probabilities of capture derived in Mitchell et al. (2019), but other potential sources of bias remain (discussed in Polansky et al. 2019). Prior population modeling in Polansky et al. (2021) using these indices identified the need for bias adjustment parameters for all juvenile and early subadult indices and for late subadult and both early and late adult indices in cohorts prior to 2001, when integrating these indices into a single analysis. Notably, the trawls used for the surveys resulting in relatively biased abundance indices were designed to sample a larger fish, age-0 striped bass (*Morone saxatilis*) (Stevens 1977), not delta smelt.

Estimates of delta smelt entrainment were developed for postlarval (Smith et al. 2020) and subadult (Smith 2019) life stages. These models accounted for uncertainty in the sequence of events leading from entrainment to observation by modeling coupled processes of transport, survival, sampling efficiency, and subsampling. Data from a coupled hydrodynamic, particle-tracking model informed a model of postlarval transport to the water diversions where postlarvae can be observed and throughout areas of the South Delta where postlarvae were unavailable for observation and not expected to survive. In contrast, the subadult and adult fish are thought to exert greater choice and control over their spatial distribution (Bennett and Burau 2015; Polansky et al. 2018; Hobbs et al. 2019). Uncertainties in subadult transport as a function of hydrodynamics led to a reduced spatial definition of subadult entrainment that only included those fish directly entrained and available for observation at the fish facilities sampling South Delta water diversions. In other words, the subadult model did not assume net flows would index the transport of older fish.

The generally accepted conceptual model for the process leading to the entrainment of delta smelt is that under conditions of low water clarity, delta smelt occupy portions of the water column that make them more vulnerable to advective flows (Grimaldo et al. 2009; Bennett and Burau 2015). Any delta smelt that happen to occupy the portion of the Delta influenced by net southward flows, towards the CVP and SWP water diversions, are at risk of entrainment into Old and Middle rivers. If they survive long enough, they may be observed by the fish collection facilities in front of the Tracy and Banks pumping plants. The CVP's Tracy Fish Facility and the SWP's Skinner Fish Facility sample a fraction of entrained fish from diverted water using behavioral louver systems (see Smith 2019 and Smith et al. 2020 for further details). Entrainment of delta smelt is managed by controlling the net reverse flow in the Old and Middle rivers (OMR; USFWS 2019; Fig. 1). Specific management criteria depend on water clarity in the South Delta, or South Delta turbidity (SDT).

Three sets of covariates were summarized: those predicting recruitment, those predicting nonentrainment-related mortality (hereinafter, natural mortality), and those predicting entrainment mortality. The recruitment and natural mortality covariates used here (Tables 1 and 2) were previously identified by Polansky et al. (2021) as those with the most evidence of having an effect in the hypothesized direction, and although the entrainment component of mortality was not explicitly modeled by Polansky et al. (2021), covariates indexing entrainment were found to be the ones most strongly associated with subadult survival. Entrainment covariates

Table 1. Delta smelt life stage transition covariates.

Life stage and data source	Modeled rate(s)	Covariate	Covariate aggregate month(s)	Covariate data source
Early postlarval (PL1); May 20 mm	Recruitment	Adult abundance	March	—
		Mean adult size	March	SMWT, SKT
	Natural mortality	None		—
	Entrainment mortality	Old and Middle river flow	April–May	USGS
		South Delta turbidity	April–May	SMWT, SKT, and 20 mm
Late post-larval (PL2); June 20-mm	Recruitment	Adult abundance	April	—
		Mean adult size	April	SKT
		Temperature	April–May	SKT and 20 mm
	Natural mortality	Outflow	June–August	Dayflow
	Entrainment mortality	Old and Middle river flow	June	USGS
		South Delta turbidity	June	20 mm and TNS
Juvenile (J); July–August TNS	Natural mortality	Delta-wide turbidity	September–November	FMWT
Early subadult (SA1); October–November FMWT	Natural mortality	Food	December–January	Neomysis–zooplankton surveys
		Age-1+ striped bass	December	FMWT
	Entrainment mortality	Old and Middle river flow	December–January	USGS
		South Delta turbidity	December–January	FMWT, SMWT, SKT
Late subadult (SA2); January–February SMWT and SKT	Natural mortality	Food	February	Neomysis–zooplankton surveys
		Age-1+ striped bass	December	FMWT
	Entrainment mortality	Old and Middle river flow	February	USGS
		South Delta turbidity	February	SMWT and SKT
Early adult (A1); March SMWT and SKT	Natural mortality	Food	March	Neomysis–zooplankton surveys
		Age-1+ striped bass	December	FMWT
	Entrainment mortality	Old and Middle river flow	March	USGS
		South Delta turbidity	March	SMWT and SKT

Note: See Table 2 for descriptions of the summary method for each covariate. Acronyms for specific delta smelt surveys are as follows: Spring Midwater Trawl Survey (SMWT), Spring Kodiak Trawl Survey (SKT), 20 mm Survey (20 mm), Summer Townet Survey (TNS), and Fall Midwater Trawl Survey (FMWT). Late adults (A2) were observed in the April SKT after 2001, but mortality of A2 was not modeled.

Table 2. Description of the summary method for each covariate used to model dynamic processes of recruitment, natural mortality, and entrainment mortality of delta smelt.

Covariate	Unit	Covariate summary details
Mean adult size	millimetre	Mean fork length observed in February 1995–2001 in the Spring Midwater Trawl Survey and 2002–2015 in the Spring Kodiak Trawl Survey
Temperature	Celsius	Mean water temperature measured by the 20 mm Survey during April to May population monitoring
Outflow	$metre^3$	Sum of the volume of water moving past a point near the confluence of the Sacramento and San Joaquin rivers, near Pittsburg, California, during June to August
Delta-wide turbidity	centimetre	Mean Secchi depth measured by the Fall Midwater Trawl Survey during September to November
Food	microgram carbon·$metre^{-3}$	Mean carbon-weighted density of adult calanoid copepods, cyclopoid copepods, cladocerans, and mysid shrimp observed during February and March zooplankton surveys
Age-1+ striped bass	Total number	Index of striped bass abundance, observed in the Fall Midwater Trawl Survey during December, excluding young of the year, calculated as $\sum_{1}^{str=15} CPUE_{str} \times volume_{str}$, where catch per unit effort (CPUE) was the mean observed in each of 15 spatial strata (str)
Old and Middle river flow	$metre^3$·$second^{-1}$	Mean of the daily sum of tidally filtered flows in the Old and Middle rivers
South Delta turbidity	centimetre	Mean Secchi depth measured by fish surveys in the southern portion of the Sacramento–San Joaquin Delta

represented the regulated metric of South Delta hydrodynamic conditions (OMR) and the environmental trigger for management action (SDT). OMR was the average of the daily sum of tidally filtered flows from two adjacent rivers, Old and Middle rivers. OMR data were available from US Geological Survey (USGS) streamflow databases (https://waterdata.usgs.gov). When streamflow data was not available to compute OMR, the Hutton model (Andrews et al. 2017) was used to estimate OMR from San Joaquin River flows and exports from South Delta water diversions. SDT, where Secchi depth indexed turbidity, was the mean of values measured during California Department of Fish and Wildlife surveys. SDT values were drawn only from locations in the southern portion of the Delta, where entrainment may affect the population. Biological data were available from ftp://ftp.dfg.ca.gov, and flow data other than OMR were available from the Dayflow database (https://data.cnra.ca.gov/dataset/dayflow).

Table 3. List of indices, parameters, and data used in the delta smelt life cycle model.

Index		
	Values	Description
i	$i = 1, 2, 3$	Entrainment covariate
s	s = PL1, PL2, J, SA1, SA2, A1, A2	Life stage
c	$c = 1995, 1996, \ldots, 2015$	Cohort year
Parameter		
	Description	Prior
$n_{AB_{sc}}$	Abundance	—
$n_{ET_{sc}}$	Number entrained	—
ρ_{sc}	Recruitment rate	—
α	Recruitment rate regression parameter	Normal(0,1)
σ_R^2	Variance of recruitment rate	Exponential(3.68)
φ_{sc}	Survival	—
M_{sc}	Instantaneous rate of natural mortality	—
β_s	Natural mortality regression parameters	Normal(−1,1.2) (intercept) Normal(0,1.2) (slope)
$\sigma_{M_s}^2$	Variance of natural mortality	Exponential(3.68)
F_{sc}	Instantaneous rate of entrainment mortality	—
γ_{is}	Entrainment mortality regression parameters	Normal(−1,1.2) (intercept) Normal(0,1.2) (slope)
σ_F^2	Variance of entrainment mortality	Exponential(3.68)
ψ_s	Bias adjustment for abundance estimate	—
Ω	Mean subadult to adult bias adjustment for entrainment estimate	Normal(0,0.31)
ω_{sc}	Bias adjustment for entrainment estimate	—
η	Regression parameter of entrainment bias adjustment model	Normal(0,0.62)
σ_B^2	Variance of entrainment bias adjustment random effect	Exponential(4.6)
Data		
	Description	
$\hat{n}_{AB_{sc}}$	Observed abundance estimate	
$\hat{\sigma}^2_{AB_{sc}}$	Variance estimate of abundance estimate	
$\hat{n}_{ET_{sc}}$	Observed entrainment estimate	
$\hat{\sigma}^2_{ET_{sc}}$	Variance estimate of observed entrainment	
$X_{R_c}, X_{M_{sc}}, X_{F_{isc}}$	Covariates predicting recruitment (R) and mortality (F and M) rates	
$m_{20mm_{sc}}$	Adjusted number of lengths >20 mm fork length in the 20 mm Survey	

Population model

State process model

Like many annual fishes, delta smelt can spawn more than once in their single spawning season (Damon et al. 2016). We modeled two recruitment events per cohort resulting in two subcohorts. The first subcohort, early postlarvae recruiting to the population in May, was produced by early adults that spawned in March, and the second subcohort, late postlarvae recruiting to the population in June, was produced by late adults that spawned in April. Late postlarval abundance was the sum of early postlarval survivors $n_{AB_{PL1c}} \times \varphi_{PL1c}$ and late adult spawning (see Table 3 for definitions of all parameters). Abundances of all subsequent life stages were nonoverlapping and modeled as the product of the prior cohort-specific life stage abundance and its survival rate φ_{sc}.

Latent abundance n_{AB} dynamics for the early postlarvae PL1, late postlarvae PL2, juveniles J, early subadults SA1, late subadults SA2, early adults A1, and late adults A2 were given by

$$(1)\qquad n_{AB_{sc}} = \begin{cases} SSB_{A1(c-1)} \times \rho_{1c} & \text{for } s = PL1 \\ n_{AB_{PL1c}} \times \varphi_{PL1c} + SSB_{A2(c-1)} \times \rho_{2c} & \text{for } s = PL2 \\ n_{AB_{(s-1)c}} \times \varphi_{(s-1)c} & \text{for } s = J,\ SA1,\ SA2,\ A1 \text{ and } A2 \end{cases}$$

where ρ_{sc} and φ_{sc} were life stage s and cohort c specific recruitment and survival functions, respectively, and the spawning stock biomass (SSB_{sc}) depended on adult abundance and mean fork length FL_{sc} converted to weight ($SSB_{sc} = 0.5 \times n_{AB_{sc}} \times 1.8 \times 10^{-6} \times FL_{sc}^{3.38}$; Kimmerer et al. 2005). Recruitment rate ρ_{sc} was modeled using lognormal distributions. Spawning by early adults, producing new recruitment observed in May (s = PL1), was modeled with a log mean parameter α_0, and spawning of late adults that produced a second recruitment observed in June (s = PL2) was modeled with log mean parameter that was a function of α_0 and mean April–May water temperature X_{R_c}:

$$(2)\qquad \rho_{sc} \sim \text{Lognormal}\begin{pmatrix} \alpha_0, \sigma_R^2 \\ \alpha_0 + \alpha_1 \times X_{R_c}, \sigma_R^2 \end{pmatrix} \quad \begin{matrix} \text{for} \quad s = PL1 \\ \text{for} \quad s = PL2 \end{matrix}$$

The model of recruitment did not include any form of density dependence (i.e., Ricker or Beverton–Holt models were not used). Following Kimmerer (2011) and Rose et al. (2013), it was assumed that modern delta smelt abundances were too low to generate intraspecific limits on vital rates or approach a carrying-capacity that could be a first-order factor in population dynamics. Further, modern abundance observations did not provide sufficient contrast between high and low population levels to inform a density-dependent model (Nobriga and Smith 2020).

The survival functions φ_{sc} explicitly described instantaneous rates of natural mortality M_{sc} and entrainment mortality F_{sc}, when entrainment occurred (s = PL1, PL2, SA1, SA2, A1), as simultaneous, competing sources of mortality:

$$\varphi_{sc} = \epsilon^{-(F_{sc}+M_{sc})} \quad (3)$$

and fixed $F_{sc} = 0$ for life stages when no entrainment was observed (s = J). The use of instantaneous rates facilitated use of Baranov's catch equation (Ricker 1975) to predict the number entrained $n_{\mathrm{ET}_{sc}}$:

$$n_{\mathrm{ET}_{sc}} = n_{\mathrm{AB}_{sc}} \times \frac{F_{sc} \times (1 - \varphi_{sc})}{(F_{sc} + M_{sc})} \quad (4)$$

M was modeled as a lognormal random variable whose expectation depended on a single covariate per life stage transition $X_{M_{sc}}$ (Tables 1 and 2), mean weight W_s, and parameters β:

$$M_{sc} \sim \mathrm{Lognormal}\left[(\beta_0 + \beta_1 \times W_s + \beta_{s+1} \times X_{M_{sc}}), \sigma^2_{M_s}\right] \quad (5)$$

The quantity $\beta_0 + \beta_1 \times W_s$ represented a stage-specific intercept that relied on the principle that natural mortality declines with body size (Lorenzen 2005; Gislason et al. 2010), and the quantity $\beta_{s+1} \times X_{M_{sc}}$ represented annual deviations from the stage-specific mean, informed by covariate $X_{M_{sc}}$. The models cited above were not expected to be accurate for delta smelt because they were all developed to approximate natural mortality for larger-bodied and longer-lived fishes, compared with delta smelt. Rather, we extended the logic that mortality was expected to decline as fish grew and estimated a delta smelt model as a linear function of mean expected weight for each life stage, W_s.

F was also modeled as a lognormal random variable with expectation that depended on OMR, SDT, and the interaction of the two, represented as covariates $X_{F_{isc}}$ (Tables 1 and 2):

$$F_{sc} \sim \mathrm{Lognormal}\left[\left(\gamma_{0,s} + \sum_{i=1}^{3} \gamma_{is} \times X_{F_{isc}}\right), \sigma^2_F\right] \quad (6)$$

We assumed that entrainment covariate effects $\gamma_{(1:3)s}$ were equal among adjacent life stages, because they were at a similar stage of development. Postlarval life stages shared entrainment slopes, and subadult and adult life stages shared slopes (i.e., $\gamma_{(1:3)\mathrm{PL1}} = \gamma_{(1:3)\mathrm{PL2}}$ and $\gamma_{(1:3)\mathrm{SA1}} = \gamma_{(1:3)\mathrm{SA2}} = \gamma_{(1:3)\mathrm{A1}}$). F_{sc} were compared with a mortality reference point, 41% of natural mortality or $0.41 \times M_{sc}$ (Zhou et al. 2012), to retrospectively assess the effectiveness of management actions taken to reduce entrainment since 1995. To account for variable M_{sc}, F_{sc} estimated for delta smelt, and the reference point was converted to proportion of deaths due to entrainment mortality, $F_{sc}/(F_{sc} + M_{sc})$ and $0.41 \times M_{sc}/(1.41 \times M_{sc})$ or 29% of total deaths.

Preliminary data analysis suggested separate process variances could not be estimated for each life stage and vital rate (i.e., two values of σ^2_R, six values of σ^2_M, and five values of σ^2_F). To overcome this, a reduced parameterization of process variances was modeled, with a single parameter σ^2_R to describe both early and late recruitment process variance and a single parameter σ^2_F to describe entrainment mortality process variance for all life stages (PL1, PL2, SA1, SA2, and A1). Two parameters ($\sigma^2_{M_s}$) described early postlarval to juvenile (PL1, PL2, and J) and early subadult to early adult (SA1, SA2, and A1) natural mortality process variance, under the assumption that environmentally driven processes in early life stages would be more stochastic than those of later life stages. Constraining process variances reduced the number of parameters to estimate from 13 to 4.

Observation model

Fish survey-based abundance indices $\hat{n}_{\mathrm{AB}_{sc}}$ and their standard errors $\widehat{\mathrm{SE}}_{\mathrm{AB}_{sc}}$ were taken from Polansky et al. (2019), and estimates of the number of fish entrained $\hat{n}_{\mathrm{ET}_{sc}}$ and the standard errors $\widehat{\mathrm{SE}}_{\mathrm{ET}_{sc}}$ were taken from Smith (2019) and Smith et al. (2020). All observations were modeled as bias-corrected lognormal random variables; that is, mean observed values, from external models, were converted to medians to parameterize the lognormal distribution by subtracting one-half variance. Given model complexity and the difficulty separating process and observation errors within a single model, we followed the approach recommended by others (Ives et al. 2003; Knape et al. 2013; Polansky et al. 2021) by fixing observation variance parameters, here as $\hat{\sigma}^2_{\mathrm{AB}_{sc}} = \log\left(1 + \widehat{\mathrm{SE}}^2_{\mathrm{AB}_{sc}}/\hat{n}^2_{\mathrm{AB}_{sc}}\right)$ and $\hat{\sigma}^2_{\mathrm{ET}_{sc}} = \log\left(1 + \widehat{\mathrm{SE}}^2_{\mathrm{ET}_{sc}}/\hat{n}^2_{\mathrm{ET}_{sc}}\right)$, during the state-space model fitting:

$$\hat{n}_{\mathrm{AB}_{sc}} \sim \mathrm{Lognormal}\left[\log(n_{\mathrm{AB}_{sc}} \times \psi_s) - \frac{\hat{\sigma}^2_{\mathrm{AB}_{sc}}}{2}, \hat{\sigma}^2_{\mathrm{AB}_{sc}}\right] \quad (7)$$

$$\hat{n}_{\mathrm{ET}_{sc}} \sim \mathrm{Lognormal}\left[\log(n_{\mathrm{ET}_{sc}} \times \omega_s) - \frac{\hat{\sigma}^2_{\mathrm{ET}_{sc}}}{2}, \hat{\sigma}^2_{\mathrm{ET}_{sc}}\right] \quad (8)$$

$\hat{n}_{\mathrm{AB}_{sc}}$ estimated from 20 mm and Spring Kodiak Trawl survey data were assumed to be unbiased measurements of the true latent states of abundance. Though some inestimable fraction of the population may be unavailable to the 20 mm and Kodak trawl gears, we assumed this fraction was negligible and did not require a bias adjustment. The $\hat{n}_{\mathrm{AB}_{sc}}$ derived from other surveys and $\hat{n}_{\mathrm{ET}_{sc}}$ derived from observations of entrained fish, on the other hand, were assumed to be biased, because a portion of the delta smelt population is systematically unavailable to the gear; therefore, bias adjustments or data integration factors were required to scale $\hat{n}_{\mathrm{AB}_{sc}}$ and $\hat{n}_{\mathrm{ET}_{sc}}$ to the abundances estimated from 20 mm and Spring Kodiak Trawl Survey data so that the observation model for all $\hat{n}_{\mathrm{AB}_{sc}}$ and $\hat{n}_{\mathrm{ET}_{sc}}$ was a function of the same latent abundance predictions (eqs. 4, 7, and 8). Relative bias adjustments ψ_s and ω_s served the same function as catchability coefficients in many fisheries stock assessment models (Arreguín-Sánchez 1996) and here can take values between 0 and 1. Preliminary modeling suggested that ψ_s and ω_s could become confounded when simultaneously estimated, so ψ_s were fixed to estimate ω_s. The ψ_s parameters were fixed at one for life stages measured by the 20 mm and Spring Kodiak surveys and fixed at the posterior means reported in Polansky et al. (2021) for other life stages, $\psi_{\mathrm{J}} = 0.42$ for the Townet Survey and $\psi_{\mathrm{SA1}} = 0.19$ for the Midwater Trawl Survey.

Life stage- and cohort-specific bias adjustment parameters ω_{sc} scaled $\hat{n}_{\mathrm{ET}_{sc}}$ to the latent entrainment predictions $n_{\mathrm{ET}_{sc}}$ to account for known biases in entrainment estimates, and ω_{sc} represented the expected fraction of the model-predicted (latent) number of entrained fish estimated by $\hat{n}_{\mathrm{ET}_{sc}}$. Postlarval observed entrainment was biased by the fraction of the population that goes unobserved; delta smelt below 20 mm fork length are not enumerated by the fish facilities monitoring South Delta entrainment because they are difficult to accurately identify. Adult observed entrainment was biased by the fraction of entrained fish that die during transport through the South Delta; no data have been collected to inform this process, so this source of loss was not included when developing subadult and adult $\hat{n}_{\mathrm{ET}}$ (Smith 2019).

Postlarval entrainment bias parameters ω_{PL1c} were estimated using length frequency data $m_{20mm_{sc}}$ collected during the 20 mm Survey, adjusted for length-based selectivity (Mitchell et al. 2019). $m_{20mm_{sc}}$ represented the number of fish observed in the 20 mm Survey between 20 and 45 mm fork length, where 45 mm was the largest possible size of a postlarval delta smelt in June, excluding larger age-1 fish. $m_{20mm_{sc}}$ were modeled as binomially distributed, with expected probability ω_{sc} and effective sample size N_{eff}:

$$(9) \qquad m_{20mm_{sc}} \sim \text{Binomial}(\omega_{sc}, N_{eff})$$

The quantity $1 - \omega_{sc}$ was the probability of encountering a fish less than 20 mm, which would not be enumerated at the fish facilities observing entrainment. Although many lengths were measured in most years, the length data was assumed to be overdispersed as a result of the potential for shoaling behavior (Bennett 2005; Davis et al. 2019). N_{eff} was therefore a smaller, unknown value compared with the total number of measured lengths. N_{eff} was estimated using the method of McAllister and Ianelli (1997) and treated as a fixed quantity in the model. In this approach, the sample size N'_{eff} was calculated that would be needed to produce the variance observed in the model fit to length data, using the fixed N_{eff} value, and the quantity $|N'_{eff} - N_{eff}|$ was iteratively minimized by changing N_{eff}. The ω_{PL1c} were modeled using logistic regression with regression parameters η. Annual variation in delta smelt hatch timing and early growth led to annual variation in ω_{PL1c}, which was represented by a normally distributed random effect θ_c:

$$(10) \qquad \omega_{PL1c} = 1/[1 + e^{-(\eta_0 + \theta_c)}], \quad \text{where } \theta_c \sim \text{Normal}(0, \sigma_B^2)$$

Late postlarvae were expected to be larger than early postlarval fish, with a greater fraction observable in the data that informed $\hat{n}_{ET_{PL2c}}$, because late postlarvae included surviving early spawned fish. In other words, $\omega_{PL2c} > \omega_{PL1c}$ and ω_{PL2c} depended on ω_{PL1c}:

$$(11) \qquad \omega_{PL2c} = 1/[1 + e^{-(\eta_0 + \eta_1 + \theta_c)}]$$

No data have been collected to directly estimate delta smelt survival in the South Delta, such as mark–recapture data, so we could not develop a parallel integrated model for subadult and adult ω_{sc}. Subadult and adult ω_{sc} were instead set equal to a single entrainment bias adjustment Ω, which was estimated using an intercept-only logistic regression model and vague regression prior.

Model fitting and diagnostics

The model was fit using JAGS (Plummer 2003) in R (R Core Team 2019) and the package R2jags (Su and Yajima 2015). All model parameters were assigned vague priors on the scale of the process of interest (i.e., hyperparameter priors were chosen so that induced survival priors were uniformly distributed; Table 3). Exponential priors for all state process standard error parameters, σ, were based on a penalized complexity prior framework (Simpson et al. 2017) and the assumption that σ exceeded a value of 1.25 with a probability less than 0.01. To our knowledge, no one has derived a set of priors for the intercept and slope parameters β and γ, so that the induced survival prior of a log–log model is uninformative. Intercept prior means were derived from the logic that if uniformed prior survival has mean 0.5, then by rearranging eq. 4, F and M intercepts must be distributed with mean log[–log(0.5)/2]. Prior standard deviations of 1.2 were found to produce a somewhat uniform induced distribution at the mean covariate values for survival purely by trial and error. A burn-in period of 20 000 iterations was followed by a posterior sample of 250 000. Convergence among six posterior chains was assessed using the Gelman–Rubin statistic (Gelman and Rubin 1992) and by examining posterior chains to see whether stationary distributions were sampled. Gelman–Rubin statistics less than 1.05 indicated model convergence. JAGS code and data to fit the delta smelt life cycle model may be found in the online Supplementary Material[1].

Regression parameters (α, β, and γ) were evaluated based on the level of evidence that a particular covariate or interaction between covariates was associated with a delta smelt vital rate. Evidence was quantified as the proportion of posterior samples that were greater than zero in instances when a positive association was hypothesized or less than zero in instances when a negative association was hypothesized. Although most entrainment and natural mortality covariates were selected based on results from a parallel modeling effort of fewer life stages (Polansky et al. 2021), we wanted to test entrainment covariates using new information (i.e., the entrainment estimates) and with a finer temporal resolution in the state process. Further, the two best subadult to adult natural mortality covariates, Food and STB1+ (see Tables 1 and 2), were not highly distinct in terms of evidence and effect size. Candidate models included those with or without OMR × SDT interactions as entrainment mortality effects, and candidate models also included either Food or STB1+ as natural mortality covariates for subadults or adults. Candidate models were compared in two stages of backwards selection using the evidence to select the best model for further inference. In the first stage, OMR × SDT interactions were evaluated based on the evidence statistic for the interaction and removed in stage 2 if not supported, with evidence less than 0.50. In the second stage, the alternate late subadult to early adult and early to late adult natural mortality covariates, Food or STB1+, were evaluated, and the covariate associated with the highest evidence statistic was selected for further inference.

Model diagnostics included leave-one-out cross-validation, checks for joint posterior correlations among model parameters, and comparison of prior and posterior distributions. Leave-one-out cross-validation was performed by sequentially omitting each individual value of $\hat{n}_{AB_{sc}}$ and $\hat{n}_{ET_{sc}}$, refitting the model, and predicting the missing observation. Cross-validation residuals (missing observation – predicted missing observation) were standardized by dividing by residual standard deviation, and the time series of cross-validation residuals were explored for values indicating poor fit (greater than 2 or less than −2) and for temporal patterns in fit. Correlation between pairwise posterior samples of all estimated model parameters (α, β, γ, σ, and ψ) was quantified by the R^2 statistic. Prior and posterior densities of all parameters were compared graphically. Posterior densities that resembled prior densities (same modal value and variance) were one indication that the parameter was not estimable with available data.

Sensitivity analyses

Assumptions were made regarding the applicability of abundance and entrainment datasets to model delta smelt population dynamics. Model sensitivity to these assumptions was tested by comparing results of a base model with results of a model with a different assumption. With reference to the model described above (the base model), a set of data and assumptions were defined, and a set of sensitivity analyses testing each data source or assumption is described below. Model sensitivity was represented as the mean proportional change of ρ and $F/(F + M)$ for each life stage, where proportional change was the difference from the base model posterior mean divided by the base model posterior mean (i.e., for a value of two and a base model value of one, proportional change = 1). Model sensitivity was also represented as the change in evidence tests from the base model, but these were represented as differences in the fractions of posterior predictions rather than proportional changes.

[1]Supplementary data are available with the article at https://doi.org/10.1139/cjfas-2020-0251.

Abundance observations $\hat{n}_{AB_{sc}}$ derived from the 20 mm and Spring Kodiak Trawl surveys were assumed to be unbiased ($\psi_s = 1$), though they may be negatively biased to the extent that shoals of delta smelt may be stochastically distributed shoreward of the trawl lanes (Bennett and Burau 2015). Model sensitivity to 20 mm Survey and Spring Kodiak Trawl Survey assumptions was tested by iteratively setting ψ_s for 20 mm- or Spring Kodiak-derived abundances to 0.75. Model sensitivity to the bias adjustments applied to Summer Townet and Midwater Trawl survey-derived abundance estimates was tested by iteratively increasing each bias adjustment by 0.5 while not changing bias adjustments for other surveys. Adult entrainment bias adjustments represented survival of entrained fish during transport. Although the entrainment observations used to fit the delta smelt life cycle model did not include this source of loss, prior modeling efforts by Kimmerer (2011) did. Dividing the life cycle model entrainment observations by entrainment estimates of Kimmerer (2011) provided an ad hoc estimate of 0.51 to fix Ω in the final sensitivity analysis.

Model projection

To explore the potential effects of entrainment mitigation on the delta smelt population and the relative effects of managing the ecosystem to reduce natural mortality, we simulated future population abundances over 3 cohort years. The simulations accounted for parameter estimate uncertainty, process variation, and covariate uncertainty. The simulation was initialized with a sample from the posterior distribution of the number of early adults in cohort year 2015. New random values for recruitment (ρ_{sc}; eq. 3) and mortality (M_{sc} and F_{sc}; eqs. 5 and 6) were simulated for each life stage and cohort year using joint posterior samples of model parameters (α, β, γ, and σ) and simulated covariate values to generate expected vital rate values.

Several future condition scenarios were considered under the assumption that future environmental conditions could be represented by simulating from distributions based on the mean and standard deviations of their values from 2007 to 2015. The first scenario represented the status quo, with all covariates varying stochastically and random OMR truncated at the current management threshold of -142 $m^3 \cdot s^{-1}$ (-5000 $ft^3 \cdot s^{-1}$). A second scenario represented the ideal Temp and Outflow (Tables 1 and 2) conditions of year 2011, a recent year of good recruitment and survival. The status quo and ideal scenarios represented lower and upper reference points to compare against alternative scenarios representing potential management actions. In other simulated scenarios, random OMR was truncated at -212 $m^3 \cdot s^{-1}$ (-7500 $ft^3 \cdot s^{-1}$) or 0 $m^3 \cdot s^{-1}$, representing greater or lower impacts of water exports on downstream entrainment processes. To test the effect of managing natural mortality, relative to management of entrainment mortality, the final simulated scenario truncated the late postlarval natural mortality covariate Outflow to eliminate values less than the lower quartile of 2007–2015 values (value observed in June–August of 2012). Truncation of Outflow in some years represented its augmentation to a minimal level. A prior delta smelt management regime (USFWS 2008) provided for conditional management of fall survival following high spring rainfall, so we simulated conditional management of Outflow following ideal spring conditions, represented by mean Temp minus one-half standard deviation. Simulated Outflow management actions occurred in ~1 of every 4 simulated years.

Covariance between environmental covariates was accounted for by simulating variables from linear regression models of 2007–2015 relationships, rather than allowing variables to vary independently. June–August Outflow was correlated with the prior April–May Temp; February Food was correlated with STB1+, and March Food was correlated with February Food. The 2007–2015 mean and standard deviation were used to simulate other covariates. The probability of population growth was equal to the proportion of joint posterior samples of projected early adult abundance that were greater than initial abundance (early adult abundance of cohort 2015), and probabilities from alternative OMR and Outflow management scenarios were compared with the status quo and ideal scenarios to evaluate the relative merits among conservation options.

Results

Life cycle models fit to 180 simulated datasets, generated from known true state parameters, demonstrated that all model parameters were estimable (see Appendix A). Depending on whether entrainment bias adjustments or entrainment observations were ignored, some parameter estimates could be biased. The entrainment mortality intercept was biased low when entrainment data were biased low, and that bias was ignored; therefore, entrainment bias adjustments were included in the delta smelt life cycle model. Entrainment bias adjustments could be estimated, but if no data were available to estimate the process associated with entrainment bias (i.e., adult delta smelt prescreen survival), the adjustments could not address interannual variation (Figs. A1–A4). Both natural mortality and entrainment mortality process variation appeared to be estimable, but at low levels of natural mortality process variation, posteriors could be dominated by the prior distribution, which manifested as low posterior shrinkage values in the simulation experiment (Figs. A3 and A4).

Specifics of the delta smelt life cycle model were developed with guidance from the simulation experiment results. Critically, all state process noise parameters appeared to be estimable, the prior distributions did not appear to result in biased parameter estimates, and entrainment bias adjustments could be estimated either with appropriate data (e.g., delta smelt postlarvae) or without observations to inform the bias adjustment (e.g., delta smelt adults and subadults).

Case study: delta smelt

Returning to the case study, delta smelt entrainment mortality of all life stages varied significantly across the 1995–2015 time series, with higher entrainment mortality estimated during the early to mid-2000s compared with the 1990s and 2007–2015 (Fig. 2). While postlarval entrainment mortality (posterior mean) only approached the 0.41 × natural mortality reference point in 2002, subadult to adult entrainment mortality exceeded the reference point during at least one life stage of the 1998–2007 (calendar years 1999–2008) cohorts, before declining to values below the reference point by the 2008 cohort. In the last years of the time series, subadult to adult entrainment mortality increased again, approaching the reference point in February and March of cohorts 2014 and 2015.

The posterior distributions of entrainment mortality parameters supported all three management hypotheses. The evidence associated with the Old and Middle river (OMR) and water clarity (South Delta turbidity, SDT) interaction was 0.91 for postlarvae (Table 4). Across all candidate models of subadult and adult natural mortality, evidence for an interactive effect of OMR and water clarity on adult entrainment was low (<0.13), so the interaction was removed in the first stage of model selection. Evidence for both OMR and SDT main effects was very high (1.00), indicating an additive effect of water clarity on adult entrainment rather than an interactive effect. Predicted entrainment mortality of all life stages was greater at low water clarity and low OMR (Fig. 3). These results supported the management hypotheses that entrainment mortality was related to OMR (F increased as OMR declined; i.e., became more negative) and that the effect of OMR depended on water clarity (F was greater when Secchi depth was low). For each life stage, the average of joint posterior entrainment mortality samples during 1999–2006 was greater than during 2007–2015, supporting the final entrainment hypothesis that entrainment mortality was reduced during the recent period of hydrodynamic management.

Effective sample size for length frequencies used to estimate postlarval entrainment bias adjustments converged on a value of 28,

Fig. 2. Time series of the proportion of deaths due to entrainment (entrainment mortality/total mortality) and associated covariates. Boxplots depict the posterior distributions of estimates, and the red lines indicate the reference point 0.41 × natural mortality, or 0.29 × total mortality (Zhou et al. 2012). Early postlarvae were observed in April–May, and late postlarvae were observed in June. Early subadults were observed in December–January, and late subadults were observed in February. Finally, early adults were observed in March. Mean entrainment covariates measured for each life stage – cohort combination are shown in the bottom two panels (see Tables 1 and 2).

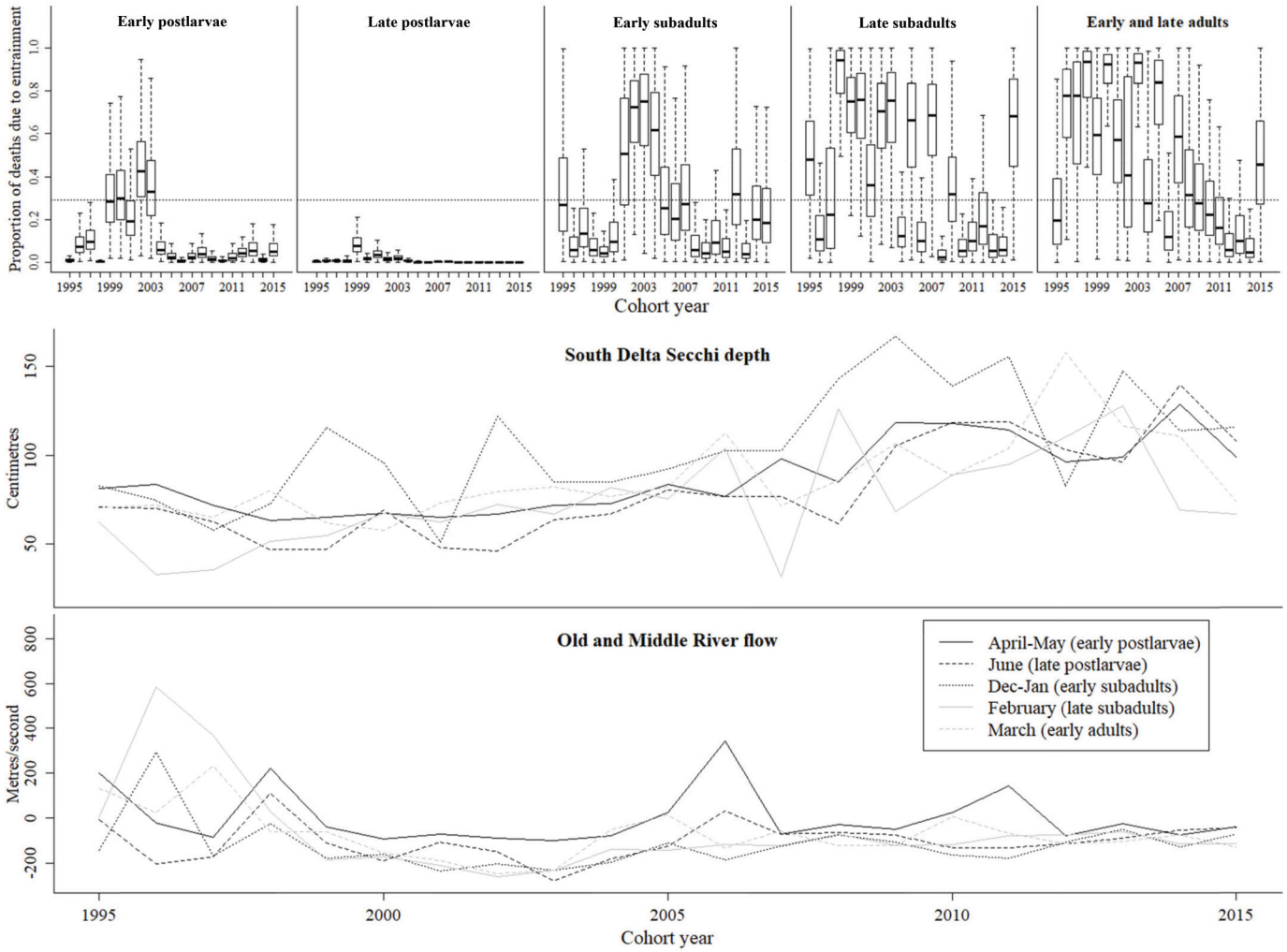

a considerable reduction from the maximum number of lengths measured during a single time period of 4322 that indicated limited information content to contrast the proportions of large and small fish. The mean posterior postlarval entrainment bias adjustments were 0.19 (95% credible interval 0.13–0.25) in April–May and 0.78 (95% credible interval 0.63–0.88) in June. The final 3 years in the time series, 2013–2015, were associated with the highest bias adjustment values (closest to 1) and highest proportions of observed lengths greater than 20 mm. The subadult to adult entrainment bias adjustment was estimated to be 0.046 (95% credible interval 0.024–0.097), suggesting that slightly less than 1 of 20 entrained subadult and adult delta smelt survive transport through the Old and Middle rivers before becoming available for observation by the fish facilities monitoring entrainment.

In addition to strong evidence for entrainment mortality, the evidence for effects from ecosystem covariates on natural mortality was high (Table 4). Recruitment of late-spawned fish was associated with average April–May water temperature. Later years 2012–2015 were warm, and recruitment of late postlarvae was lower relative to most of the earlier years (Fig. 4). Natural mortality of late postlarvae was associated with mean June–August Outflow. As Outflow declined over the time series, estimated mortality of postlarvae during June to August increased significantly. Natural mortality of juveniles during September to November was negatively associated with Delta-wide Turbidity, but the associated evidence was relatively low (0.70). Between age-1+ striped bass (STB1+) and prey density (Food) covariates, STB1+ evidence was highest for early subadults, and Food evidence was highest for late subadults and adults. STB1+ (SA1 life stage) and Food (SA2 and A1 life stage) were therefore selected as the best natural mortality covariates for further inference. Natural mortality of early subadults was positively associated with STB1+, which was highest in the 1990s, declined in the 2000s, and increased again in the 2010s. Natural mortality of late subadults and adults was negatively associated with Food, which generally declined over the study period, resulting in somewhat greater mortality during the spawning period. Most variation in late subadult and adult natural mortality, however, appeared to be lost in process noise, as demonstrated by wide and overlapping 95% credible intervals of the mortality estimates.

Diagnostics

Results from the cross-validation exercise demonstrated random scatter around 0 for all abundance and entrainment residuals

Table 4. Posterior evidence (proportion of posterior distributions greater or less than 0) for all modeled covariate effects.

Process (month)	Covariate	Evidence			
Stage 1: Compare subadult with adult entrainment interactions, at four configurations of subadult to adult natural mortality					
Subadult to adult entrainment mortality (February–March)	Old and Middle river flow × South Delta Secchi depth	0.102	0.128	0.129	0.108
Stage 2: Compare subadult with adult natural mortality covariates					
Early subadult natural mortality (December–January)	Age-1+ striped bass	0.942	0.914	—	—
	Food	—	—	0.704	0.634
Late subadult to adult natural mortality (February–March)	Age-1+ striped bass	—	0.323	0.384	—
	Food	0.984	—	—	0.972
Stage 3: Refit model with no subadult to adult entrainment interaction, Age-1+ striped bass as an early subadult natural mortality covariate, and Food as late subadult to adult natural mortality covariate					
Late recruitment (June)	Water temperature	0.977	—	—	—
Late postlarval natural mortality (June–August)	Outflow	0.987	—	—	—
Postlarval entrainment mortality (April–June)	South Delta Secchi depth	1.000	—	—	—
	Old and Middle river flow	1.000	—	—	—
	Old and Middle river flow × South Delta Secchi depth	0.914	—	—	—
Juvenile mortality (September–November)	Secchi depth	0.699	—	—	—
Early subadult natural mortality (December–January)	Age-1+ striped bass	0.936	—	—	—
Late subadult to adult natural mortality (February–March)	Food	0.983	—	—	—
Subadult to adult entrainment mortality (February–March)	South Delta Secchi depth	1.000	—	—	—
	Old and Middle river flow	1.000	—	—	—

Note: Candidate models are indicated by each column, and rows show different stages of model selection. Only evidence for interactions is presented for subadult entrainment mortality in Stage 1. Water temperature, Old and Middle river flow, South Delta Secchi depth, Outflow, and Food (see Tables 1 and 2) were each hypothesized to have negative effects on the corresponding vital rate, and all others were hypothesized to have positive effects. Only one natural mortality effect was applied to each life stage (Stage 2), and only the model supported in Stages 1 and 2 was explored in Stage 3. Some covariate effects were therefore not applicable (denoted with a long dash, —).

(missing observation – predicted missing value; Fig. 5). Cross-validation residuals were very small for entrainment observations, because high entrainment observation error resulted in high residual standard deviation. On the other hand, 15 of 140 abundance cross-validation residuals were greater than 2 or less than −2, indicating poor fit of 11% of model predictions to the missing abundance observations. Relative to entrainment, abundance observation errors were lower, resulting in lower residual standard deviation and larger standardized abundance residual values. Fit to two abundance observations were particularly poor. The early postlarval observation in May 2005 and the early subadult observation in 1995 were much lower than predicted by the life cycle model. Some joint posterior correlation was evident between the intercept and weight coefficients of the natural mortality model (eq. 5; Fig. A5) and between the early subadult entrainment mortality intercept (eq. 6) and subadult entrainment bias, but the next highest joint posterior correlation was low (R^2 = 0.18). Posteriors of all model parameters converged on stationary distributions (Fig. A6) and moved away from their prior distributions (Fig. A7), indicating that the parameters were informed by the delta smelt abundance and entrainment data.

Sensitivity analysis

The relative values of F and M were sensitive to assumptions about abundance and entrainment observations, but the evidence tests on posterior distributions of regression coefficients were not (Table 5). Assuming a negative bias in 20 mm-derived abundance observations led to lower $F/(F + M)$ for postlarval life stages, but assuming negative bias in Spring Kodiak-derived abundance observations had little effect on $F/(F + M)$ of any life stage. $F/(F + M)$ for later life stages was sensitive to assumptions about the bias of the Summer Townet Survey. Assuming less bias in Summer Townet-derived abundance observations led to higher $F/(F + M)$ for subadult and adult life stages. Model estimates of F were extremely sensitive to the entrainment bias adjustments. Assuming a value of 0.51 for subadults and adults, versus 0.05 estimated by the model, using a vague prior, resulted in ∼90% lower $F/(F + M)$. Recruitment rates ρ were most sensitive to the assumptions that 20 mm-derived abundance observations were unbiased and that the externally derived Townet Survey bias adjustment (ψ_J = 0.42) was correct.

Population projection

In the ideal conditions scenario, represented by year 2011 Temp and Outflow, probabilities of population growth over 3 years were at least 0.81 (Table 6). A status quo scenario, with OMR set to $-142\ m^3 \cdot s^{-1}$ and an environment varying with the 2007–2015 mean and standard deviation, resulted in a probability of 0.39 of population growth. The difference in probability of population growth between a status quo OMR and a relatively high OMR (socioeconomically infeasible) management scenario (OMR = 0) was 3.6%, and the difference between random and managed Outflow scenarios was only ∼0.4%. Among all simulated scenarios, only simulations of year 2011 conditions resulted in greater than 0.5 probability of population growth.

Discussion

Management of delta smelt has operated under the hypotheses that entrainment mortality resulting from operation of the CVP and SWP in the South Sacramento–San Joaquin Delta is a function of the net flow in the Old and Middle rivers (OMR) and that this effect is greater when water clarity is low. In agreement with previous research (Grimaldo et al. 2009; Kimmerer 2011; Polansky et al. 2021), the model developed here supported these hypotheses. OMR and a measure of water clarity were each related to entrainment mortality at all affected life stages, supporting the management of entrainment risk using a combination of OMR

Fig. 3. Posterior distributions of predicted entrainment mortality at two levels of water clarity (2007–2015 interquartile range) and a range of Old and Middle river flows. The dark shaded regions indicate the interquartile range of posterior predictions, and the light shaded regions indicate the 95% credible intervals. The dotted horizontal lines indicate the reference point 0.41 × natural mortality, or 0.29 × total mortality (Zhou et al. 2012).

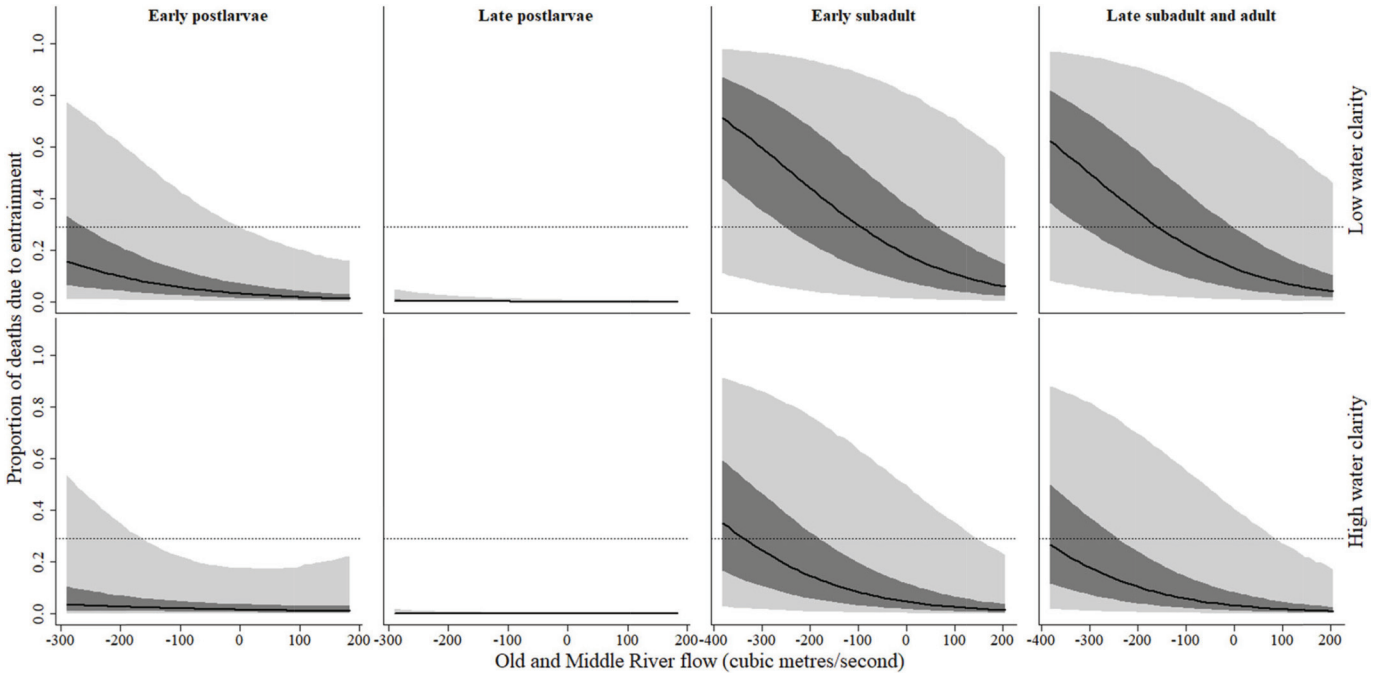

Fig. 4. Time series of recruitment success, estimates of natural mortality, and associated covariates. Boxplots depict the posterior distributions of recruitment and mortality estimates, and red lines show the corresponding covariates. The late postlarval recruitment covariate was measured in April–May, and June–August ecosystem conditions were related to late postlarval natural mortality. Juvenile natural mortality was indexed by September–November conditions, and early subadult covariates were measured in December–January. Finally, February and March covariates were related to late subadult and adult natural mortality (see Tables 1 and 2).

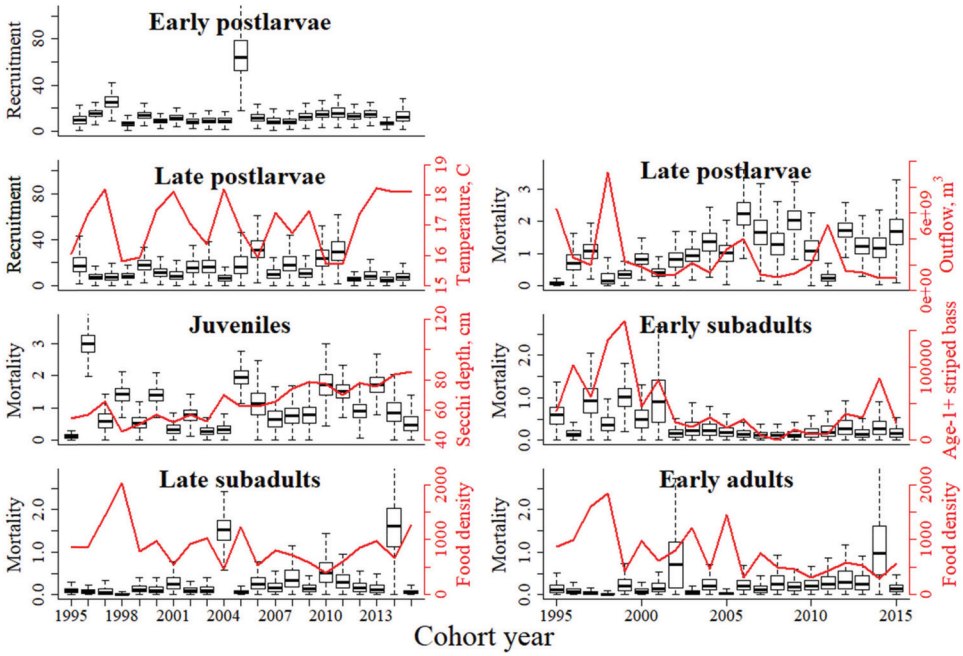

Fig. 5. Standardized residuals from leave-one-out cross-validation, where residuals equal the differences between the missing observations and the predicted missing values. Residuals were standardized by dividing by residual standard deviation within each life stage and type of observation. Abundance residuals are shown in the top row, and entrainment residuals are shown in the bottom row.

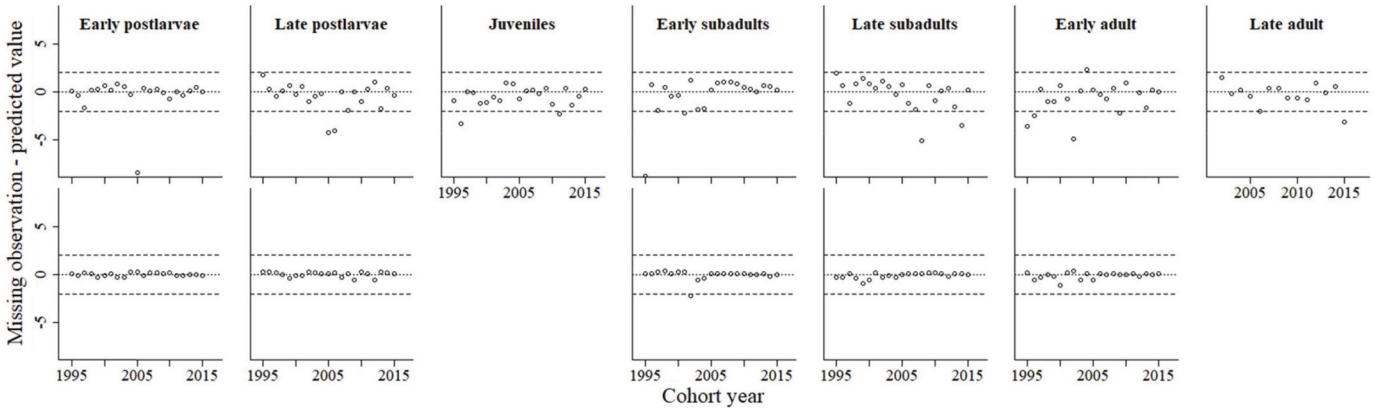

Table 5. Results of sensitivity analysis, showing proportional changes from the base model when a single aspect of the model was altered.

	1.5 × 20 mm-derived	1.5 × Spring Kodiak-derived	Summer Townet bias adjustment	Fall Midwater Trawl bias adjustment	Adult entrainment bias adjustment
Proportional change in vital rates					
$F_{PL1}/(F_{PL1} + M_{PL1})$	**−0.298**	−0.012	−0.046	−0.073	0.038
$F_{PL2}/(F_{PL2} + M_{PL2})$	**−0.329**	0.008	−0.114	−0.051	−0.017
$F_{SA1}/(F_{SA1} + M_{SA1})$	−0.018	0.022	**0.277**	−0.064	**−0.913**
$F_{SA2}/(F_{SA2} + M_{SA2})$	0.015	−0.031	**0.257**	−0.087	**−0.868**
$F_{A1}/(F_{A1} + M_{A1})$	0.017	−0.059	**0.221**	−0.126	**−0.880**
ρ_{PL1}	**0.346**	−0.170	−0.012	0.182	0.004
ρ_{PL2}	**0.366**	−0.194	−0.037	0.187	−0.020
Change in evidence					
Water temperature (April–May)	−0.012	0.004	−0.023	−0.001	0.011
Outflow (June–August)	−0.001	0.003	−0.008	0.002	0.004
Turbidity (September–November)	−0.005	0.111	−0.064	0.191	0.015
Age 1+ striped bass (December–January)	0.000	−0.022	−0.016	−0.016	0.015
Food (February–March)	0.002	0.003	0.012	0.000	0.050
OMR × Turbidity (April–June)	−0.002	−0.001	−0.006	0.002	−0.002
OMR (December–March)	0.000	0.000	0.000	0.000	0.000
Turbidity (December–March)	0.000	0.000	0.000	0.000	0.000

Note: For parameter definitions, see Table 3. Vital rate sensitivity was summarized as the mean proportional change across each life stage. Sensitivity values greater than an absolute value of 0.2 are bolded.

Table 6. Three-year projected probabilities of population growth under different environmental and hydrodynamic conditions.

	Probability of population growth		
Old and Middle river flow ($m^3 \cdot s^{-1}$)	Random summer outflow	Avoid lowest outflow after a cold spring	Best year of recent temperatures and outflow (2011)
−212	0.385	0.389	0.813
−142	0.387	0.390	0.815
0	0.423	0.426	0.841

thresholds and water clarity triggers. In agreement with Polansky et al. (2021), who found effects of OMR on recruitment, the effects of these covariates were supported in early life stages as well as later life stages.

The final entrainment management hypothesis addressed by the model was that the management regime beginning in 2007 was associated with a decrease in entrainment mortality. Entrainment mortality appeared to vary by three time periods that were associated with different management of OMR flow. During 1995–1998, no management threshold was applied to OMR, but several consecutive high rainfall, high OMR years occurred (Fig. 2). Highly variable OMR during this early period was associated with highly variable entrainment mortality. During 1999–2005, Delta water exports were managed to a low OMR (less than −142 $m^3 \cdot s^{-1}$), resulting in the highest entrainment mortality for all life stages. Finally, since 2007, water exports have usually been managed to an OMR threshold of no less than −142 $m^3 \cdot s^{-1}$, and entrainment mortality was lowest for all life stages after calendar year 2007.

The time period 1995–2015 was characterized by several long-term trends in the upper San Francisco Estuary that were quantitatively linked to patterns in delta smelt recruitment and mortality. Important trends in late winter to early summer ecosystem conditions were increasing abundance of juvenile striped bass and declining prey density, associated with greater winter mortality, and declining outflow, associated with greater summer mortality. Though not increasing appreciably over 1995–2015, late spring water temperature was elevated for an extended duration during the historic 2013–

2016 drought in California, and this was associated with poor recruitment success of late spawned delta smelt for several years in a row. A long-term trend towards a drier (Reis et al. 2019), hotter Delta (Dettinger et al. 2015), dominated by exotic food items, predators, and competitors (Sommer et al. 2007; Brown et al. 2016), is a likely driver of ecosystem conditions that will increase delta smelt mortality and lower recruitment success.

Limitations of model and data

In addition to the effect of management, there may be additional causes of the long-term decline in estimated entrainment mortality that could not be modeled with currently available information. South Delta water clarity has increased over time, contributing to the long-term decline in entrainment mortality, but important variation in South Delta ecosystem dynamics could not be modeled. Changes to the South Delta habitat and predator field were ignored, because temporal variation in mortality during the transport of entrained fish was not explicitly modeled (Smith 2019; Smith et al. 2020). Decreasing delta smelt occupancy of the Lower San Joaquin River due to declining turbidity and a changing fish community may also contribute to the long-term decline in entrainment mortality. It is important to consider the biological meaning of the entrainment covariates that were modeled. Entrainment into the South Delta is an inherently spatial process, because it occurs in a specific location in the Delta and is not continuously applied across the full spatial distribution of the delta smelt population. Fish only become vulnerable to entrainment when they happen to occupy the portion of the Delta where advective flows (OMR) may draw them into the South Delta, and this vulnerability is enhanced by low water clarity. Thus, the OMR covariate should be considered an index of the force acting on fish in a location somewhere in the San Joaquin River near its confluence with the Sacramento River. If fish are located elsewhere and do not occupy these areas, hydrodynamic modeling suggests water export should have less effect (Kimmerer and Nobriga 2008).

The power to detect water clarity effects and interactions may have been greater for earlier life stages because of the data used to develop postlarval entrainment observations. As postlarvae were assumed to be passively transported, hydrodynamic data, including the variables that determine OMR (San Joaquin River flow and water export volume), were used to estimate the transport of postlarvae through the South Delta. In effect, OMR was encoded in postlarval entrainment observations, leaving greater power for the life cycle model to detect other effects. If future data to model-observed entrainment of later life stages include the transport of fish as a function of hydrodynamics and behavior, similar improvements to the power to detect interactive effects may be realized for subadult and adult life stages.

The modeling approach we employed relied on abundance and entrainment bias adjustments (i.e., data integration parameters) to scale survey-specific sets of observations to the true latent abundance of the population. Although the model was sensitive to each of these parameters, sensitivity analyses demonstrated that the model was extremely sensitive to the entrainment bias adjustments. The postlarval bias adjustment accounted for entrainment of fish below 20 mm fork length that are too small to be enumerated at the fish facilities sampling entrained fishes, and data were available to model this bias in the form of observed length frequencies. The adult entrainment bias adjustment accounted for transport through the Old and Middle rivers and the losses associated with this transport, which, unlike postlarvae, were not directly modeled in the observations. During transport through the Old and Middle rivers, delta smelt may be lost to predation or transported to regions where they become geographically isolated from the population. Observed postlarval entrainment accounted for transport and survival, because postlarval transport could be modeled like a passive particle using a coupled hydrodynamic particle tracking model (Kimmerer 2011; Smith et al. 2020). Adults, however, are thought to exhibit behaviors that modulate their hydrodynamic transport through the Delta (Bennett and Burau 2015). As these behaviors have not been quantified at spatial scales relevant to the entrainment process, adult transport could not be modeled as a function of hydrodynamics, and no data currently exist to directly estimate predation rates or validate the indirect value we estimated (the subadult to adult entrainment bias adjustment, Ω). Simulation testing revealed that this parameter could be estimated indirectly, as we did in the delta smelt life cycle model, but annual variation could not be accounted for. Future mark–recapture experiments in the Old and Middle rivers could provide data to directly estimate the survival of entrained delta smelt during transport and an adult entrainment bias adjustment.

Abundance observations derived from the 20 mm and Spring Kodiak Trawl surveys were assumed to be unbiased, but these abundance observations could be biased to the extent that some fish are systematically unavailable to be sampled by survey gears or evade the approaching nets. In contrast with entrainment observations that are biased in known ways, the direction of abundance biases is unclear. For example, large trawl gears like those used by the 20 mm and Spring Kodiak Trawl surveys are suited to sampling pelagic habitats but not littoral habitats, and delta smelt residing in littoral habitats are unavailable to these surveys. Limited information suggests that delta smelt vertical and lateral distribution may be affected by tidal phase (Bennett et al. 2002; Bennett and Burau 2015; Feyrer et al. 2013; Polansky et al. 2018), generating additional potential sources of bias for the open-water trawl indices. Sensitivity analyses demonstrated that if 20 mm and Spring Kodiak Trawl survey-derived abundances were biased and were systematically underestimated, then the relative contribution of entrainment to total mortality ($F/(F + M)$) could be over- or underestimated, depending on the life stage.

Although the delta smelt life cycle model presented here addressed the management of delta smelt entrainment using the hydrodynamic covariate OMR, the active management of OMR occurs at a much finer temporal scale than we were able to model for delta smelt population dynamics. While OMR is actively managed at a subweekly scale, it is necessary to aggregate delta smelt observations at the monthly or bimonthly scale to avoid severe zero inflation. Delta smelt became increasingly rare and difficult to detect over the time period modeled. The temporal mismatch between hydrodynamic management and population modeling means that the delta smelt life cycle model will have limited utility to guide day-to-day management of delta smelt entrainment. Rather, it can be used to guide long-term planning and management at a coarser, life-stage-specific scale. Simulations of delta smelt hydrodynamic transport and behavior (Gross et al. 2017) in the South Delta may provide more insight into subweekly variation in entrainment risk.

Management implications

Previous examples of life cycle models to estimate simultaneous rates of mortality were applied to harvested populations (Rochette et al. 2013; Massiot-Granier et al. 2014; Cadigan 2015; Miller et al. 2016). The goal of such models is commonly to calculate a target harvest mortality rate that will lead to sustainable harvest or the rate of harvest mortality that balances recruitment and natural mortality (Ricker 1975; Zhou et al. 2012). Current delta smelt entrainment management appears to have limited postlarval entrainment mortality to a small fraction of mean natural mortality (less than 8.6% estimated here). Though declining substantially during the initial years of the current management regime (2007–2008), the fraction of subadult to adult mortality attributable to entrainment increased in the later years of the time series (2014–2015), possibly to levels that are expected to harm the population (equaling or exceeding natural mortality in

February and March of cohort 2015 (calendar year 2016)). Although entrainment management has attempted to reduce specific life stage mortalities, a primary management concern is that population growth rates have not increased under the current management regime. In a population in which recruitment success rates cannot sustain the population, no additional mortality is sustainable; there is no surplus production. Given average environmental conditions, no level of predicted delta smelt entrainment mortality, including that associated with zero net OMR, led to a high probability of population growth. No additional mortality can be sustained by the population, but that does not mean that entrainment mortality of 0 will result in its recovery. Entrainment mortality cannot be completely eliminated because water exports must continue; thus, the question of a target level of entrainment mortality becomes a subjective policy question. How much attrition are policy-makers willing to accept?

Although low mean delta smelt recruitment rates preclude the estimation of a traditional reference point (RFP), derived from sustainable fishing theory, alternative RFPs can be derived from estimates of natural mortality. We applied the lower mortality RFP estimated by Zhou et al. (2012) (0.41 × natural mortality) to retrospectively evaluate delta smelt entrainment mortality. As it is based on fishing theory and the assumption that the population could compensate for entrainment losses, this RFP does not represent a recovery target for delta smelt. Rather, 0.41 × natural mortality represents a point beyond which we could be certain of harm to the population. We recommend that management for population recovery strive for a high probability of avoiding the RFP.

Entrainment mortality of delta smelt during the late 1990s and early 2000s was extremely high, exceeding the RFP, especially for subadult and adult life stages. Entrainment was the dominant factor in mortality for these later life stages during this period and was likely a factor in declining abundance at that time. With the revised management of delta smelt entrainment beginning in 2007 (USFWS 2008), entrainment mortality appeared to decline for several years, before increasing and approaching the RFP again in the terminal year (January–March of calendar year 2016). These results suggest that changes in regulatory application in response to extreme drought and variation in environmental conditions (e.g., more predators and less food) in 2016 reduced the effectiveness of OMR management.

The 2008 and 2019 USFWS Biological Opinions specified two classes of management actions. Actions to limit entrainment losses in the winter and spring and an action to limit juvenile mortality was specified for the fall in 2008 and summer–fall in 2019. As previously stated, entrainment is managed by monitoring hydrodynamic and environmental conditions and actively limiting advective flows into the South Delta. The delta smelt life cycle model indicated that entrainment actions were successful in reducing mortality, supporting status quo water operations, and results suggested that new or modified management actions may be necessary to improve the odds that the population will recover. Population projections using the fitted delta smelt life cycle model, however, suggested a low probability of population growth under any modeled scenario. A pessimistic implication of this result is that the limited manipulation of the Delta ecosystem that is possible to support delta smelt will have a low probability of achieving growth in the population.

Although none of the scenarios we tested resulted in projected population growth, the conditions tested were admittedly not comprehensive, and many others are possible (i.e., some scenarios we did not consider could lead to greater probabilities of population growth). Results did, however, suggest that some management strategies could have greater potential for limiting mortality than others. Active management of entrainment appears to have been successful in reducing mortality, though entrainment management alone did not appear to be sufficient to recover the population. In addition to entrainment, other sources of mortality may be managed by augmenting seasonal ecosystem conditions, but the delta smelt population projections indicated that even combined actions may be insufficient. In recognition of the limits within which the San Francisco Estuary may be actively managed, recent management plans for delta smelt include supplementation of the wild population with hatchery-origin fish (USFWS 2019).

A prior management strategy for delta smelt (USFWS 2008) provided for limitation of juvenile mortality during certain years of high winter and spring outflow, when enhanced survival may sustain population growth until the next spawning season. Limitation of juvenile mortality may be accomplished by maintaining sufficient outflow to keep the low salinity zone westward of the confluence of the Sacramento and San Joaquin rivers where turbidity is often higher and water temperatures are cooler. Such a positioning of the low salinity zone is considered to maximize available delta smelt habitat during a demographic bottleneck — poor growth and high mortality. Although the results here demonstrate significant variation in juvenile (fall) mortality during the years 1995–2015, most variation appeared to occur prior to 2007. In subsequent years, juvenile mortality was less variable and was significantly less than mortality experienced earlier in the year by postlarvae. This result suggests that ecosystem management to eliminate delta smelt demographic bottlenecks would be more effective earlier in the year.

An alternative conclusion is that substantial observation error associated with juvenile and early subadult delta smelt life stages precluded the finding of any significant variation in juvenile mortality during later years. Juvenile delta smelt were observed in the Townet Survey, and early subadults were observed in the Fall Midwater Trawl Survey. Neither gear nor survey design were devised to sample delta smelt, and their capacity to produce an index of the delta smelt population with adequate precision is questionable (Polansky et al. 2019). A recently developed US Fish and Wildlife Service survey for delta smelt, the Enhanced Delta Smelt Monitoring Program, has had greater success capturing delta smelt during this seasonal period and may reveal more about mortality during the summer and fall.

We modeled late postlarval natural mortality as a function of mean June–August Outflow, which may be considered an index of many Delta ecosystem conditions, including the multivariate habitat suitability of the low salinity zone (Bever et al. 2016) and prey availability (e.g., R^2 = 0.86 and 0.70, respectively, for June–August, 1995–2015). Model projections indicated that conditions at the limits of recent ranges in ecosystem conditions may be required for growth of the delta smelt population (e.g., the exceptional conditions of year 2011). Under warming climate conditions and greater demand for Central Valley water (Dettinger et al. 2015; Reis et al. 2019), such conditions are likely to manifest less frequently in the future. The effect mechanisms implied by the best-supported covariates may need to be mitigated with focused conservation efforts, if it is possible to do so. It is possible that conditions for higher recruitment success and summer survival can be provided without extreme weather. For example, the California Department of Water Resources is currently experimenting with summer prey enhancement by rerouting the flow of water in the northern Delta (Frantzich et al. 2018; Sommer et al. 2020).

Conclusions

The framework of the state-space model was particularly useful for the delta smelt population, because it was necessary to separate a very noisy signal from very noisy observations. The state-space model explicitly separated process variation from observation error, accounting for more variation in observations than a process or observation error only model. In many instances, observation errors manifested as disagreement from one survey to the next; abundance observations increased in later life stages. Latent abundances estimated by the life cycle model smoothed over these differences, improving vital rate-covariate inferences.

The noisy delta smelt signal was further compartmentalized into distinct sources of mortality, facilitating comparisons among categories of management actions. The model adds to the growing evidence that multiple, simultaneously acting mortality rates may be estimated when observations of the number of mortalities are combined with observations of abundance in a population model. A common approach to fitting population models, especially in fisheries stock assessments, is to assume that natural mortality cannot be estimated and set it to a constant, externally estimated value, but evidence from hierarchical modeling indicates that more information about natural mortality rates can be derived from harvest and abundance data than was previously recognized (Millar and Meyer 2000; Miller and Hyun 2018). Using simulations, we demonstrated that it was possible to extract both entrainment and natural mortality rates, coefficients, and process variance (see Appendix A). Consistent with the findings of Aanes et al. (2007), however, we found that natural mortality process variance was still a difficult parameter to estimate, especially when the true value was relatively low. A useful approach would integrate additional data, such as mark–recapture data, to further inform the natural mortality model (Cadigan 2015), but to date this has not been possible for delta smelt due to their small size, rarity, and limited artificial production.

Hierarchical models, such as integrated models and state-space models, have the potential to disentangle complex biological relationships and provide quantitative guidance to conserve and manage populations. Partitioning parameter, process, and observation uncertainties facilitates probabilistic assessments of the risk associated with management actions. The delta smelt life cycle model presented here provided a basis to compare the relative effects of different actions focused on different life stages, and it will be used to evaluate the risk associated with a range of water export operations. Though it is common practice for fish populations, formulation of survival rates in terms of multiple sources of mortality is not common outside of fisheries science. We expect the model presented here will have greater utility in management of other populations where abundance and the number of mortalities due to a particular source can be estimated (Smallwood 2007; Servanty et al. 2010).

Acknowledgements

The findings and conclusions in this article are those of the authors and do not necessarily represent the views of the US Fish and Wildlife Service, the Department of Interior, or the other member agencies of the Interagency Ecological Program for the San Francisco Estuary (IEP). Li-Ming He and two anonymous reviewers kindly provided comments on early drafts of this manuscript. Lara Mitchell did much of the work to compile and summarize data, and Ken B. Newman initiated and led the delta smelt life cycle model project for many years. His role was critical in model development and conceptualization. Funding was provided by the California Department of Water Resources and the US Bureau of Reclamation. The research presented here relied extensively on data provided by the IEP.

References

Aanes, S., Engen, S., Sæther, B.E., and Aanes, R. 2007. Estimation of the parameters of fish stock dynamics from catch-at-age data and indices of abundance: can natural and fishing mortality be separated? Can. J. Fish. Aquat. Sci. **64**(8): 1130–1142. doi:10.1139/f07-074.

Andrews, S.W., Gross, E.S., and Hutton, P.H. 2017. Modeling salt intrusion in the San Francisco Estuary prior to anthropogenic influence. Cont. Shelf Res. **146**: 58–81. doi:10.1016/j.csr.2017.07.010.

Arreguín-Sánchez, F. 1996. Catchability: a key parameter for fish stock assessment. Rev. Fish. Biol. Fish. **6**(2): 221–242. doi:10.1007/BF00182344.

Bennett, W.A. 2005. Critical assessment of the delta smelt population in the San Francisco Estuary, California. SFEWS, **3**(2). doi:10.15447/sfews.2005v3iss2art1.

Bennett, W.A., and Burau, J.R. 2015. Riders on the storm: selective tidal movements facilitate the spawning migration of threatened Delta Smelt in the San Francisco Estuary. Estuar. Coasts, **38**(3): 826–835. doi:10.1007/s12237-014-9877-3.

Bennett, W.A., Kimmerer, W.J., and Burau, J.R. 2002. Plasticity in vertical migration by native and exotic estuarine fishes in a dynamic low-salinity zone. Limnol. Oceanogr. **47**(5): 1496–1507. doi:10.4319/lo.2002.47.5.1496.

Bever, A.J., MacWilliams, M.L., Herbold, B., Brown, L.R., and Feyrer, F.V. 2016. Linking hydrodynamic complexity to Delta smelt (*Hypomesus transpacificus*) distribution in the San Francisco estuary, U.S.A. SFEWS, **14**(1). doi:10.15447/sfews.2016v14iss1art3.

Brown, L.R., Kimmerer, W.J., and Brown, R. 2009. Managing water to protect fish: a review of California's environmental water account, 2001–2005. Environ. Manage. **43**(2): 357–368. doi:10.1007/s00267-008-9213-4. PMID:18830738.

Brown, L.R., Kimmerer, W.J., Conrad, J.L., Lesmeister, S., and Mueller–Solger, A. 2016. Food webs of the Delta, Suisun Bay, and Suisun Marsh: an update on current understanding and possibilities for management. SFEWS, **14**(3). doi:10.15447/sfews.2016v14iss3art4.

Cadigan, N.G. 2015. A state-space stock assessment model for northern cod, including under-reported catches and variable natural mortality rates. Can. J. Fish. Aquat. Sci. **73**(2): 296–308. doi:10.1139/cjfas-2015-0047.

Cloern, J.E., and Jassby, A.D. 2012. Drivers of change in estuarine-coastal ecosystems: Discoveries from four decades of study in San Francisco Bay. Rev. Geophys. **50**(4). doi:10.1029/2012RG000397.

Damon, L.J., Slater, S.B., Baxter, R.D., and Fujimura, R.W., 2016. Fecundity and reproductive potential of wild female Delta Smelt in the upper San Francisco Estuary, California. Calif. Fish Game 102: 188–210. Available from https://pdfs.semanticscholar.org/5e26/fc359ef439b1a2c30a4367428e4f17eb2d66.pdf.

Davis, B.E., Hansen, M.J., Cocherell, D.E., Nguyen, T.X., Sommer, T., Baxter, R.D., et al. 2019. Consequences of temperature and temperature variability on swimming activity, group structure, and predation of endangered delta smelt. Freshw. Biol. **64**(12): 2156–2175. doi:10.1111/fwb.13403.

de Valpine, P., and Rosenheim, J.A. 2008. Field-scale roles of density, temperature, nitrogen, and predation on aphid population dynamics. Ecology, **89**(2): 532–541. doi:10.1890/06-1996.1. PMID:18409442.

Dettinger, M., Udall, B., and Georgakakos, A. 2015. Western water and climate change. Ecol. Appl. **25**: 2069–2093. doi:10.1890/15-0938.1. PMID:26910940.

Feyrer, F., Portz, D., Odum, D., Newman, K.B., Sommer, T., Contreras, D., et al. 2013. SmeltCam: Underwater video codend for trawled nets with an application to the distribution of the imperiled delta smelt. PLoS ONE, **8**: e67829. doi:10.1371/journal.pone.0067829. PMID:23861814.

Frantzich, J., Sommer, T., and Scheier, B. 2018. Physical and biological responses to flow in a tidal freshwater slough complex. SFEWS, **16**(1). doi:10.15447/sfews.2018v16iss1/art3.

Gelman, A., and Rubin, D.B. 1992. Inference from iterative simulation using multiple sequences. Statist. Sci. **7**(4): 457–511. doi:10.1214/ss/1177011136.

Gislason, H., Daan, N., Rice, J.C., and Pope, J.G. 2010. Size, growth, temperature and the natural mortality of marine fish. Fish Fish. **11**(2): 149–158. doi:10.1111/j.1467-2979.2009.00350.x.

Grimaldo, L.F., Sommer, T., Van Ark, N., Jones, G., Holland, E., Moyle, P.B., et al. 2009. Factors affecting fish entrainment into massive water diversions in a tidal freshwater estuary: can fish losses be managed? N. Am. J. Fish. Manage. **29**(5): 1253–1270. doi:10.1577/M08-062.1.

Gross E.S., Saenz, B., Rachiele, R., Grinbergs, S., Grimaldo, L.F., Korman, J., et al. 2017. Estimation of adult delta smelt distribution for hypothesized swimming behaviors using hydrodynamic, suspended sediment and particle-tracking models. Resource Management Associates, Davis, Calif. Collaborative and Adaptive Management Team, Study 2 Technical Report.

Harwood, J., and Stokes, K. 2003. Coping with uncertainty in ecological advice: lessons from fisheries. Trends Ecol. Evol. **18**(2): 617–622. doi:10.1016/j.tree.2003.08.001.

Hobbs, J.A., Lewis, L.S., Willmes, M., Denney, C., and Bush, E. 2019. Complex life histories discovered in a critically endangered fish. Sci. Rep. **9**: 1–12. doi:10.1038/s41598-019-52273-8. PMID:30626917.

Ives, A.R., Dennis, B., Cottingham, K., and Carpenter, S.R. 2003. Estimating community stability and ecological interactions from time-series data. Ecol. Monogr. **73**(2): 301–330. doi:10.1890/0012-9615(2003)073[0301:ECSAEI]2.0.CO;2.

Kimmerer, W.J. 2011. Modeling Delta Smelt losses at the south Delta export facilities. SFEWS, **9**(1): Article 3. doi:10.15447/sfews.2011v9iss1art3.

Kimmerer, W.J., and Nobriga, M.L. 2008. Investigating particle transport and fate in the Sacramento–San Joaquin Delta using a particle-tracking model. SFEWS, **6**(1). doi:10.15447/sfews.2008v6iss1art4.

Kimmerer, W.J., and Rose, K.A. 2018. Individual-based modeling of delta smelt population dynamics in the Upper San Francisco Estuary III. Effects of entrainment mortality and changes in prey. Trans. Am. Fish. Soc. **147**(5): 223–243. doi:10.1002/tafs.10015.

Kimmerer, W.J., Avent, S.R., Bollens, S.M., Feyrer, F.V., Grimaldo, L.F., Moyle, P.B., et al. 2005. Variability in length–weight relationships used to estimate biomass of estuarine fish from survey data. Trans. Am. Fish. Soc. **134**(2): 481–495. doi:10.1577/T04-042.1.

Knape, J., Besbeas, P., and de Valpine, P. 2013. Using uncertainty estimates in analyses of population time series. Ecology, **94**(9): 2097–2107. doi:10.1890/12-0712.1. PMID:24279280.

Lande, R. 1993. Risks of population extinction from demographic and environmental stochasticity and random catastrophes. Am. Nat. **142**(6): 911–927. doi:10.1086/285580. PMID:29519140.
Lorenzen, K. 2005. Population dynamics and potential of fisheries stock enhancement: practical theory for assessment and policy analysis. Philos. Trans. R. Soc. Lond. B. Biol. Sci. **360**(1453): 171–189. doi:10.1098/rstb.2004.1570. PMID:15713596.
Mangel, M., MacCall, A.D., Brodziak, J., Dick, E.J., Forrest, R.E., Pourzand, R., and Ralston, S. 2013. A perspective on steepness, reference points, and stock assessment. Can. J. Fish. Aquat. Sci. **70**(6): 930–940. doi:10.1139/cjfas-2012-0372.
Massiot-Granier, F., Prévost, E., Chaput, G., Potter, T., Smith, G., White, J., et al. 2014. Embedding stock assessment within an integrated hierarchical Bayesian life cycle modelling framework: an application to Atlantic salmon in the Northeast Atlantic. ICES J. Mar. Sci. **71**(7): 1653–1670. doi:10.1093/icesjms/fst240.
Maunder, M.N., and Deriso, R.B. 2011. A state–space multistage life cycle model to evaluate population impacts in the presence of density dependence: illustrated with application to delta smelt (*Hyposmesus transpacificus*). Can. J. Fish. Aquat. Sci. **68**(7): 1285–1306. doi:10.1139/f2011-071.
McAllister, M.K., and Ianelli, J.N. 1997. Bayesian stock assessment using catch-age data and the sampling – importance resampling algorithm. Can. J. Fish. Aquat. Sci. **54**(2): 284–300. doi:10.1139/f96-285.
McGill, B.J., Dornelas, M., Gotelli, N.J., and Magurran, A.E. 2015. Fifteen forms of biodiversity trend in the Anthropocene. Trends Ecol. Evol. **30**(2): 104–113. doi:10.1016/j.tree.2014.11.006. PMID:25542312.
Meyer, R., and Millar, R.B. 1998. Bayesian stock assessment using a nonlinear state-space model. Stat. Model. **1998**: 284–291.
Millar, R.B., and Meyer, R. 2000. Bayesian state-space modeling of age-structured data: fitting a model is just the beginning. Can. J. Fish. Aquat. Sci. **57**(1): 43–50. doi:10.1139/f99-169.
Miller, W.J. 2011. Revisiting assumptions that underlie estimates of proportional entrainment of delta smelt by state and federal water diversions from the Sacramento–San Joaquin Delta. SFEWS, **9**(1). doi:10.15447/sfews.2011v9iss1art2.
Miller, T.J., and Hyun, S.Y. 2018. Evaluating evidence for alternative natural mortality and process error assumptions using a state-space, age-structured assessment model. Can. J. Fish. Aquat. Sci. **75**(5): 691–703. doi:10.1139/cjfas-2017-0035.
Miller, W.J., Manly, B.F., Murphy, D.D., Fullerton, D., and Ramey, R.R. 2012. An investigation of factors affecting the decline of delta smelt (*Hypomesus transpacificus*) in the Sacramento–San Joaquin Estuary. Rev. Fish. Sci. **20**(1): 1–19. doi:10.1080/10641262.2011.634930.
Miller, T.J., Hare, J.A., and Alade, L.A. 2016. A state-space approach to incorporating environmental effects on recruitment in an age-structured assessment model with an application to southern New England yellowtail flounder. Can. J. Fish. Aquat. Sci. **73**(8): 1261–1270. doi:10.1139/cjfas-2015-0339.
Mitchell, L., Newman, K.B., and Baxter, R. 2019. Estimating the size selectivity of fishing trawls for short-lived fish species. SFEWS, **17**(1). doi:10.15447/sfews.2019v17iss1art5.
Moyle, P.B. 2002. Inland fishes of California: revised and expanded. University of California Press, Berkeley, California, USA.
Moyle, P.B., Hobbs, J.A., and Durand, J.R. 2018. Delta smelt and water politics in California. Fisheries, **43**(1): 42–50. doi:10.1002/fsh.10014.
Newman, K.B. 1998. State-space modeling of animal movement and mortality with application to salmon. Biometrics, **54**(4): 1290–1314. doi:10.2307/2533659.
Nobriga, M.L., and Smith, W.E. 2020. Did a Shifting Ecological Baseline Mask the Predatory Effect of Striped Bass on Delta Smelt? SFEWS, **18**(1): 1–27. doi:10.15447/sfews.2020v18iss1art1.
Plummer, M. 2003. JAGS: a program for analysis of Bayesian graphical models using Gibbs sampling. *In* Proceedings of the 3rd International Workshop on Distributed Statistical Computing, Vienna, Austria.
Polansky, L., Newman, K.B., Nobriga, M.L., and Mitchell, L. 2018. Spatiotemporal models of an estuarine fish species to identify patterns and factors impacting their distribution and abundance. Estuar. Coasts, **41**: 572–581. doi:10.1007/s12237-017-0277-3.
Polansky, L., Mitchell, L., and Newman, K.B. 2019. Using multistage design-based methods to construct abundance indices and uncertainty measures for delta smelt. Trans. Am. Fish. Soc. **148**(4): 710–724. doi:10.1002/tafs.10166.
Polansky, L., Newman, K.B., and Mitchell, L. 2021. Improving inference for nonlinear state-space models of animal population dynamics given biased sequential life stage data. Biometrics, **2020**: 1–10. doi:10.1111/biom.13267.
R Core Team, 2019. R: A language and environment for statistical computing. R Foundation for Statistical Computing, Vienna, Austria. Available from https://www.R-project.org/.
Reis, G.J., Howard, J.K., and Rosenfield, J.A. 2019. Clarifying Effects of Environmental Protections on Freshwater Flows to—and Water Exports from—the San Francisco Bay Estuary. SFEWS, **17**(1): Article 1. doi:10.15447/sfews.2019v17iss1art1.
Ricker, W.E. 1975. Computation and interpretation of biological statistics of fish populations. Vol. 191. Department of the Environment, Fisheries and Marine Service, Ottawa, Ontario, Canada.
Rochette, S., Le Pape, O., Vigneau, J., and Rivot, E. 2013. A hierarchical Bayesian model for embedding larval drift and habitat models in integrated life cycles for exploited fish. Ecol. Appl. **23**(7): 1659–1676. doi:10.1890/12-0336.1. PMID:24261047.
Rose, K.A., Kimmerer, W.J., Edwards, K.P., and Bennett, W.A. 2013. Individual-based modeling of delta smelt population dynamics in the upper San Francisco Estuary: I. Model description and baseline results. Trans. Am. Fish. Soc. **142**: 1238–1259. doi:10.1080/00028487.2013.799518.
Servanty, S., Choquet, R., Baubet, É., Brandt, S., Gaillard, J.M., Schaub, M., et al. 2010. Assessing whether mortality is additive using marked animals: a Bayesian state–space modeling approach. Ecology, **91**(7): 1916–1923. doi:10.1890/09-1931.1. PMID:20715610.
Simpson, D., Rue, H., Riebler, A., Martins, T.G., and Sørbye, S.H. 2017. Penalising model component complexity: a principled, practical approach to constructing priors. Stat. Sci. **32**(1): 1–28. doi:10.1214/16-STS576.
Smallwood, K.S. 2007. Estimating wind turbine-caused bird mortality. J. Wildlife Manage. **71**(8): 2781–2791. doi:10.2193/2007-006.
Smith, W.E. 2019. Integration of transport, survival, and sampling efficiency in a model of South Delta entrainment. SFEWS, **17**(4). doi:10.15447/sfews.2019v17iss4art4.
Smith, W.E., Newman, K.B., and Mitchell, L. 2020. A Bayesian hierarchical model of postlarval delta smelt entrainment: integrating transport, length composition, and sampling efficiency in estimates of loss. Can. J. Fish. Aquat. Sci. **77**(5): 789–813. doi:10.1139/cjfas-2019-0148.
Sommer, T., Armor, C., Baxter, R., Breuer, R., Brown, L., Chotkowski, M., et al. 2007. The collapse of pelagic fishes in the upper San Francisco Estuary. Fish. **32**(6): 270–277. doi:10.1577/1548-8446(2007)32[270:TCOPFI]2.0.CO;2.
Sommer, T., Hartman, R., Koller, M., Koohafkan, M., Conrad, J.L., MacWilliams, M., et al. 2020. Evaluation of a large-scale flow manipulation to the upper San Francisco Estuary: response of habitat conditions for an endangered native fish. PLoS ONE, **15**(10): e0234673. doi:10.1371/journal.pone.0234673. PMID:33002006.
Stevens, D.E. 1977. Striped bass (*Morone saxatilis*) monitoring techniques in the Sacramento–San Joaquin Estuary. *In* Proceedings of the Conference on Assessing the Effects of Power-Plant-Induced Mortality on Fish Populations. pp. 91–109. doi:10.1016/B978-0-08-021950-9.50014-4.
Su, Y.S., and Yajima, M., 2015. R2jags: Using R to Run 'JAGS'. Version 0.5-7. Available from https://CRAN.R-project.org/package=R2jags.
USFWS. 2008. Biological opinion on the long-term operational criteria and plan for coordination of the Central Valley Project and State Water Project. United States Fish and Wildlife Service (USFWS). Available from https://www.fws.gov/sfbaydelta/CVP-SWP/index.htm.
USFWS. 2019. Biological opinion for the reinitiation of consultation on the coordinated operations of the Central Valley Project and State Water Project. United States Fish and Wildlife Service (USFWS). Available from https://www.fws.gov/sfbaydelta/cvp-swp/documents/10182019_ROC_BO_final.pdf.
Vitousek, P.M., Mooney, H.A., Lubchenco, J., and Melillo, J.M. 1997. Human domination of Earth's ecosystems. Science, **277**(5325): 494–499. doi:10.1126/science.277.5325.494.
Whipple, A.A., Grossinger, R.M., Rankin, D., Stanford, B., and Askevold, R. 2012. Sacramento–San Joaquin Delta historical ecology investigation: Exploring pattern and process. San Francisco Estuary Institute-Aquatic Science Center, Richmond, California, USA.
Williams, B.K. 2011. Adaptive management of natural resources—framework and issues. J. Environ. Manage. **92**(5): 1346–1353. doi:10.1016/j.jenvman.2010.10.041.
Zhou, S., Yin, S., Thorson, J.T., Smith, A.D., and Fuller, M. 2012. Linking fishing mortality reference points to life history traits: an empirical study. Can. J. Fish. Aquat. Sci. **69**(8): 1292–1301. doi:10.1139/f2012-060.

Appendix A

Simulation model to test the performance of the state-space life cycle model

The estimability of life cycle model parameters was explored using a simulation study. We hoped to resolve the following questions about inference of the model:

1. whether two mortality intercepts and process variances could be simultaneously estimated,
2. whether the model was estimable across a range of process noise variances,
3. whether the priors resulted in biased parameter estimates, and
4. whether entrainment bias adjustments were estimable from the type of information available for delta smelt.

True values of state parameters were simulated using Monte Carlo methods to draw 180 random values from the prior distributions used in model fitting. From each of these 180 simulated sets of

true state parameters, population abundances and observations were simulated over a 20-year time series. Finally, the model was iteratively refit to each of these simulated datasets, and the properties of posterior parameter distributions were evaluated.

State process model

The simulation model was a slightly simplified version of the model fit to the delta smelt data. See Table 3 of the main text for parameter descriptions. Reproduction, natural mortality, and entrainment mortality were simulated among five life stages: postlarvae, juveniles, early and late subadults, and adults (eq. A1). Postlarvae were produced by the previous cohort's adults (eqs. A2 and A3), and some postlarvae died due to natural mortality as fish aged into the juvenile class (eqs. A4 and A5). Entrainment of juvenile through adult life stages occurred, so transitions to early subadult and adult life stages were functions of entrainment and natural mortality. Recruitment success, natural mortality, and entrainment mortality were modeled as functions of covariates $X_{R_{sc}}$, $X_{M_{sc}}$, and $X_{F_{sc}}$, respectively (eqs. A3, A5, and A6), each of which was generated from a Normal(0,1) distribution. A single natural mortality process noise variance parameter and a single entrainment mortality process noise variance parameter was shared across all life stages. Entrainment predictions were calculated using the Baranov catch equation (eq. A7).

$$\text{(A1)} \qquad n_{\mathrm{AB}_{sc}} = \begin{bmatrix} n_{\mathrm{PL}c} \\ n_{\mathrm{J}c} \\ n_{\mathrm{SA1}c} \\ n_{\mathrm{SA2}c} \\ n_{\mathrm{A}c} \end{bmatrix}$$

$$\text{(A2)} \qquad n_{\mathrm{AB}_{sc}} = \begin{cases} n_{\mathrm{A}(c-1)} \times \rho_c & \text{for} \quad s = \mathrm{PL} \\ n_{(s-1)c} \times \varphi_{(s-1)c} & \text{for} \quad s = \mathrm{J},\ \mathrm{SA1},\ \mathrm{SA2},\ \text{and A} \end{cases}$$

$$\text{(A3)} \qquad \rho_{sc} \sim \mathrm{Lognormal}\left(\alpha_0 + \alpha_1 \times X_{R_{sc}}, \sigma_R^2\right)$$

$$\text{(A4)} \qquad \varphi_{sc} = \begin{cases} \mathrm{e}^{-(M_{sc})} & \text{for} \quad s = \mathrm{PL} \\ \mathrm{e}^{-(F_{sc}+M_{sc})} & \text{for} \quad s = \mathrm{J},\ \mathrm{SA1},\ \text{and SA2} \end{cases}$$

$$\text{(A5)} \qquad M_{sc} \sim \mathrm{Lognormal}\left(\beta_0 + \beta_s \times X_{M_{sc}}, \sigma_M^2\right)$$

$$\text{(A6)} \qquad F_{sc} \sim \mathrm{Lognormal}\left(\gamma_0 + \gamma_1 \times X_{F_{sc}}, \sigma_F^2\right) \quad \text{for } s = \mathrm{J},\ \mathrm{SA1}, \mathrm{SA2},\ \text{and A}$$

$$\text{(A7)} \qquad n_{\mathrm{ET}_{sc}} = n_{\mathrm{AB}_{sc}} \times \frac{F_{sc} \times (1 - \varphi_{sc})}{(F_{sc} + M_{sc})}$$

Entrainment bias model

Entrainment biases were estimated from simulated length frequencies m_{sc} for juvenile and early subadult life stages (eqs. A8–A10) and from a simulated variable q representing the survival of entrained fish for late subadults and adults (eq. A11). Though no data have been collected to estimate delta smelt survival after entrainment, future information from mark–recapture experiments could inform eq. A11.

$$\text{(A8)} \qquad m_{sc} \sim \mathrm{Binomial}(\omega_{sc}, N)$$

$$\text{(A9)} \qquad \begin{aligned} \mathrm{logit}(\omega_{sc}) &= \eta_0 + \theta_c \quad \text{for } s = \mathrm{J} \text{ and} \\ \mathrm{logit}(\omega_{sc}) &= \eta_0 + \eta_1 + \theta_c \quad \text{for } s = \mathrm{SA1} \end{aligned}$$

$$\text{(A10)} \qquad \theta_c \sim \mathrm{Normal}\left(0, \sigma_{B_1}^2\right)$$

$$\text{(A11)} \qquad q_j \sim \mathrm{Normal}\left(\Omega, \sigma_{B_2}^2\right) \quad \text{where } \omega_{sc} = 1/(1 + \mathrm{e}^{-\Omega}) \quad \text{for } s = \mathrm{SA2 \text{ and } A}$$

Observation model

From simulated values of abundance and entrainment, observations $\hat{n}_{\mathrm{AB}_{sc}}$ and $\hat{n}_{\mathrm{ET}_{sc}}$ were randomly simulated from lognormal distributions (eqs. A12 and A13). Lognormal standard errors for observations were fixed at 0.3 for abundance observations and 0.5 for entrainment observations. Observed entrainment was biased low to reflect delta smelt entrainment prediction bias, so observations were adjusted by a bias factor ω, which scaled the true entrainment down to the observed value needed for data integration:

$$\text{(A12)} \qquad \hat{n}_{\mathrm{AB}_{sc}} \sim \mathrm{Lognormal}\left[\log(n_{\mathrm{AB}_{sc}}) - \frac{\hat{\sigma}^2_{\mathrm{AB}_{sc}}}{2}, \hat{\sigma}^2_{\mathrm{AB}_{sc}}\right]$$

$$\text{(A13)} \qquad \hat{n}_{\mathrm{ET}_{sc}} \sim \mathrm{Lognormal}\left[\log(n_{\mathrm{ET}_{sc}} \times \omega_s) - \frac{\hat{\sigma}^2_{\mathrm{ET}_{sc}}}{2}, \hat{\sigma}^2_{\mathrm{ET}_{sc}}\right]$$

Estimation model

The estimation model was identical to the operating model described above. In other words, in the absence of observation error, estimated model parameters would be distributed around the true values as long as all parameters were estimable. In the estimation model, all vital rate parameters (α, β, and γ) were assigned vague priors, and all process noise variance parameters (σ_R^2, σ_M^2, σ_F^2, and σ_B^2) were assigned penalized complexity priors, assuming a 0.01 probability that error exceeded a value of 1.25 (Simpson et al. 2017).

For each iteration of the simulation, a set of true values was drawn and a set of stochastic observations of abundance and entrainment were simulated. Four variations of the observation model, representing different potential modeling approaches, were fit to the same observations. The first observation model (OM1) did not use $\hat{n}_{\mathrm{ET}_{sc}}$ observations and did not attempt to separate F and M. In this case, entrainment effects $\gamma_1 \times X_{F_{sc}}$ were included with the model of M (eq. A5). The second observation model (OM2) did separate F and M, but did not include simulated data m_{sc} or q_j when estimating entrainment bias adjustment terms (eqs. A8–A11). A mean value, with a Uniform(0,1) prior distribution, was estimated for juvenile to early subadult life stages, and a second mean value was estimated for late subadults and adults. The third observation model (OM3) was based on the full model described above but did not include an entrainment bias adjustment parameter ω (i.e., ω was fixed at 1). The fourth observation model (OM4) represented the full model described above, including estimation of F and, critically, estimation of ω by integrating additional simulated information.

All simulations and model fitting were performed using JAGS (Plummer 2003) and R statistical package R2jags (Su and Yajima 2015). To sample posterior distributions from the fitted model, a burn-in period of 5000 was followed by 25 000 samples of posterior distributions. The posterior distributions of all state transition parameters and process variance parameters were compared with the true simulated values using the z score (i.e., (posterior mean – true value)/posterior standard deviation) and 95% credible interval coverage of the true value. z scores and coverages explored potential biases in posteriors; the dispersion of posterior distributions was evaluated by comparing posterior standard deviations with prior standard deviations with the posterior shrinkage statistic (1 – posterior standard deviation/prior standard deviation). Posterior shrinkage near 1 indicated that observations strongly informed model parameters, while

Table A1. 95% credible interval coverage of all model parameters, among models fit to 180 simulated datasets.

	Parameter	Ignore entrainment observations (OM1)	Ignore bias adjustment data (OM2)	Ignore entrainment bias adjustment (OM3)	Full model (OM4)
Starting n_{AB}		0.95	0.95	0.93	0.96
Reproduction	α_0	0.95	0.95	0.95	0.96
	α_1	0.98	0.96	0.97	0.96
Natural mortality	β_0	0.53	0.95	0.70	0.91
	β_1	0.86	0.96	0.89	0.96
	β_2	0.78	0.96	0.86	0.96
	β_3	0.73	0.97	0.86	0.97
Entrainment mortality	η_0	—	—	—	0.92
	η_1	—	—	—	0.94
	η_2	—	—	—	0.95
	Mean ω_1	—	0.96	—	—
	Mean ω_2	—	0.99	—	—
	Mean ω_3	—	0.97	—	—
	γ_0	—	0.97	0.03	0.96
	γ_1	0.41	0.95	0.88	0.96
Process variation	σ_F	—	0.92	0.60	0.96
	σ_M	0.82	0.98	0.92	0.97
	σ_R	0.95	0.96	0.95	0.93
	σ_{B_1}	—	—	—	0.97
	σ_{B_2}	—	—	—	0.96

Fig. A1. Posterior mean versus true simulated values for reproductive (alpha) and process noise variance (sigma) parameters and starting abundance parameters. The dotted reference line indicates a one-to-one relationship.

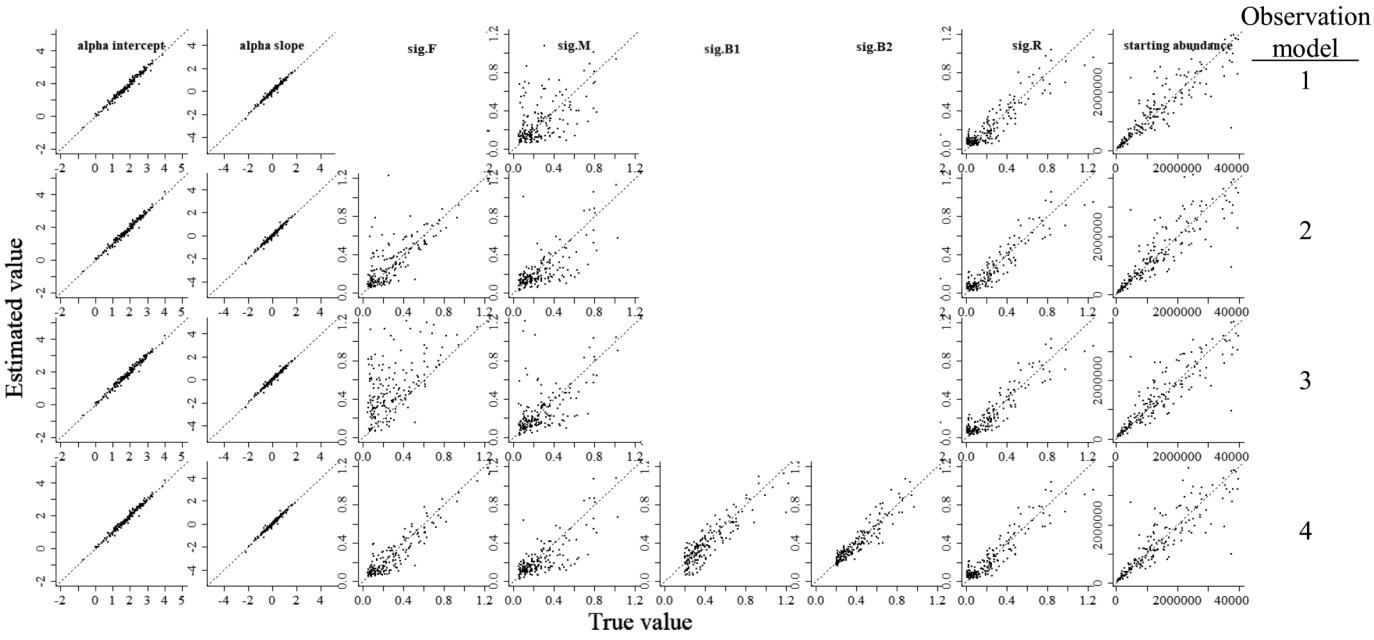

posterior shrinkage near 0 indicated that data poorly informed parameters (Betancourt 2018). Bias was also evaluated graphically by plotting posterior means versus true values.

Results and discussion

With the full observation model (OM4) that included entrainment bias adjustment parameters, entrainment bias observations, and entrainment observations, all vital rate and process noise variance parameters appeared to be estimable (Table A1; Figs. A1 and A2). This was true across a range of potential true states and parameter values and using the priors used to fit the life cycle model to delta smelt. Posterior 95% coverage of the true value was greater than 0.9 for all parameters, and the true value was almost always contained within 95% credible intervals of the posterior (Table A1).

Fig. A2. Results from simulation test showing posterior mean versus true simulated values for natural mortality (beta), entrainment bias adjustment (eta (model with random effects) or omega (model with no random effect)), and entrainment mortality (gamma). The dotted reference line indicates a one-to-one relationship.

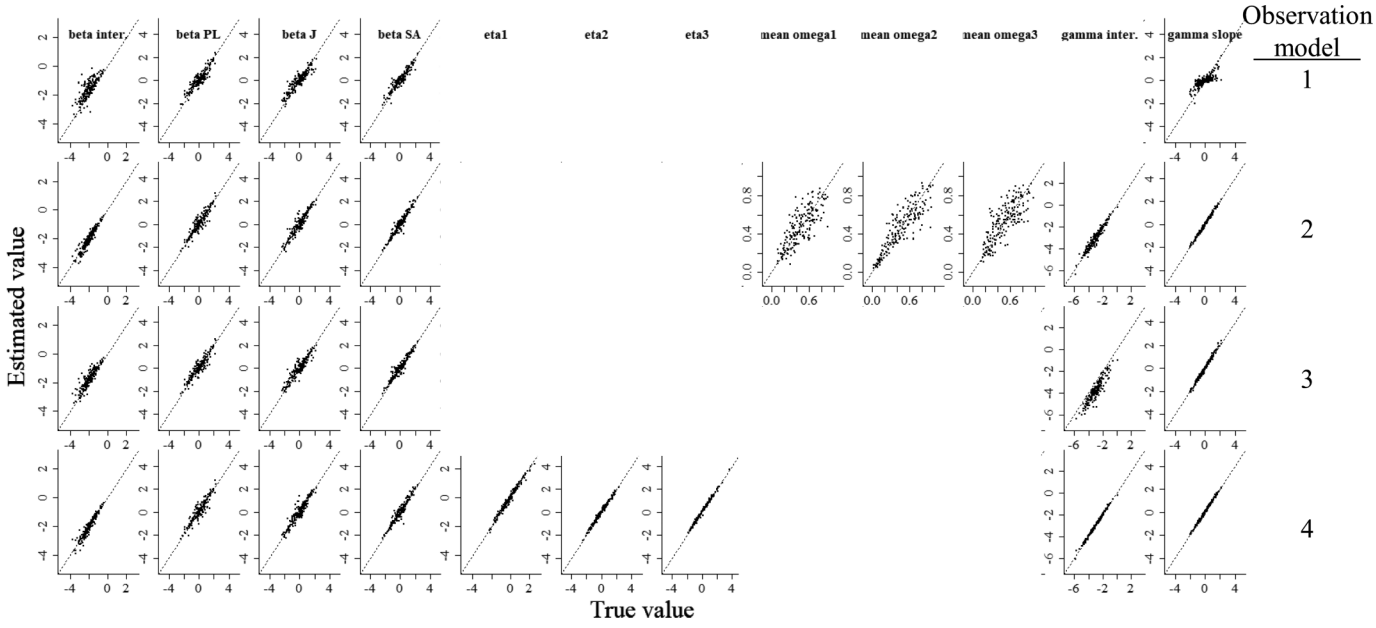

Fig. A3. Results from simulation test depicting central tendency versus dispersion of posterior distributions for reproductive (alpha) and process noise variance (sigma) parameters and starting abundance parameters. Central tendency is represented by bias (*z* score), and dispersion is represented by the contraction of posteriors from prior distributions (posterior shrinkage).

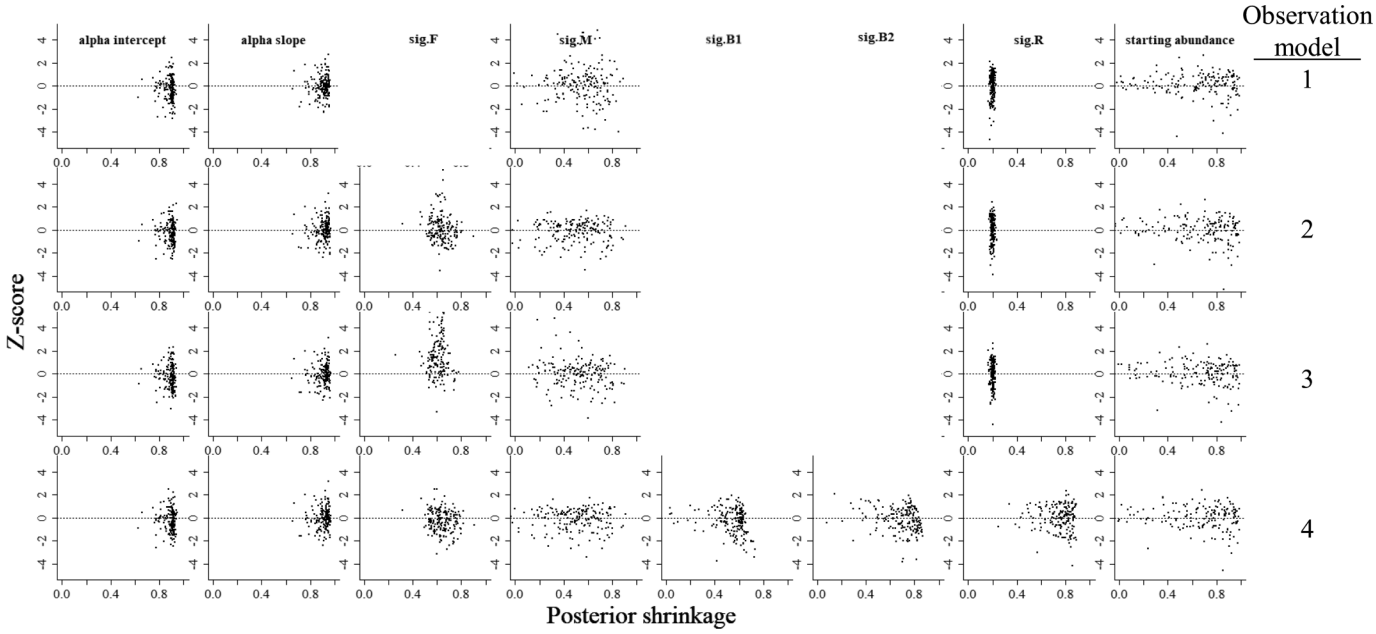

Posterior means were evenly distributed around true values with no apparent biases (Figs. A1 and A2).

When entrainment observations were ignored (OM1), however, posterior 95% coverage of mortality and process variance parameters declined (Table A1), entrainment mortality slope parameters were biased towards 0 (Fig. A2), natural mortality process variation was not well-estimated (Fig. A1), and entrainment process variation was not separately estimable. Posterior 95% coverage of most parameters was also lower when the model was fit using entrainment observations but the entrainment bias was ignored (OM3), and ignoring entrainment bias resulted in negative bias in posterior means of the entrainment mortality intercept parameter. Surprisingly, a mean entrainment bias adjustment was estimable even when entrainment bias observations were ignored (OM2), though annual variation was not accounted for, leading to greater error in entrainment mortality variance.

Relationships between posterior shrinkage and bias (*z* score) were consistent across the four modeling scenarios explored (Figs. A3

Fig. A4. Results from simulation test depicting central tendency versus dispersion of posterior distributions for natural mortality (beta), entrainment bias adjustment (eta (model with random effects) or omega (model with no random effect)), and entrainment mortality (gamma). Central tendency is represented by bias (*z* score), and dispersion is represented by the contraction of posteriors from prior distributions (posterior shrinkage).

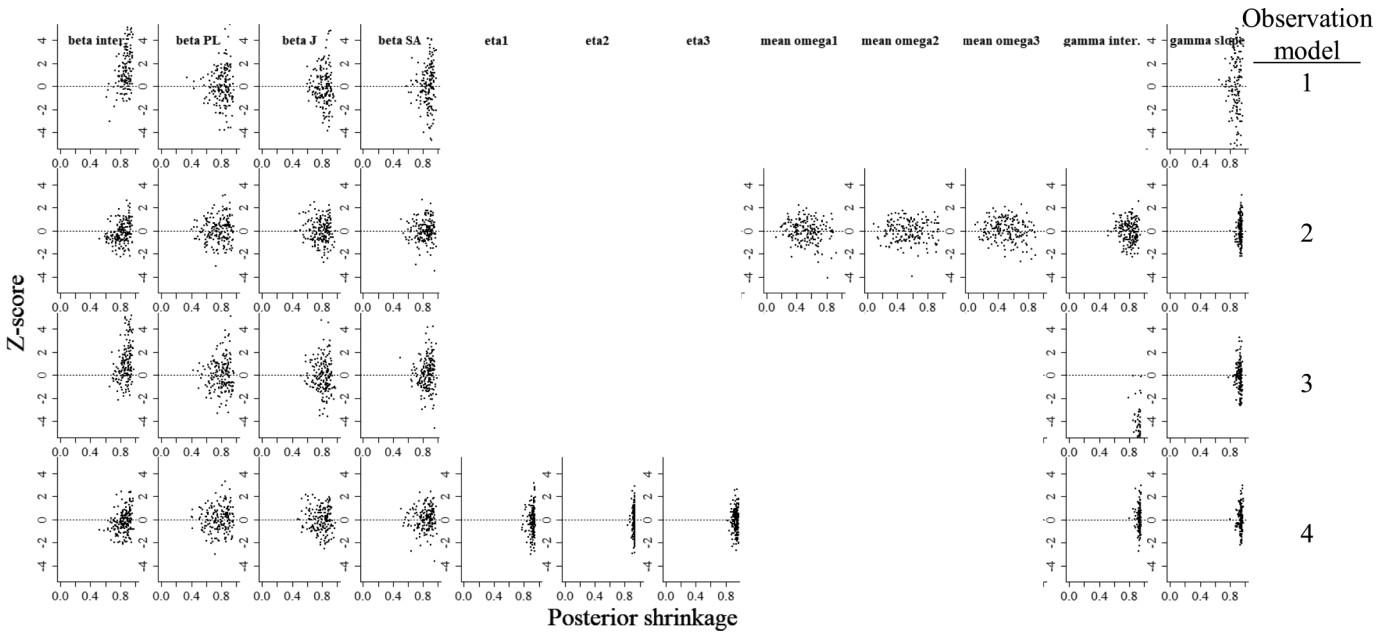

Fig. A5. The greatest two joint posterior correlations between delta smelt life cycle model parameters (R^2 = 0.37 (top panel) and 0.59 (bottom panel)). *F* is entrainment mortality, and *M* is all other mortality.

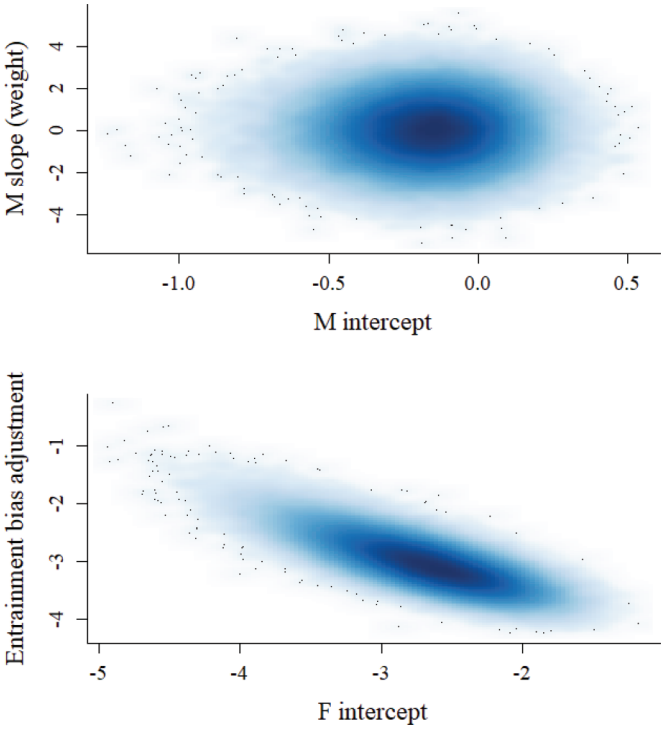

Fig. A6. Posterior traceplots of all regression coefficients for recruitment success (alpha), other mortality (*M*) intercept model, other mortality slopes (beta), entrainment mortality (gamma), and process errors (sig). Lines of different colors represent six posterior chains.

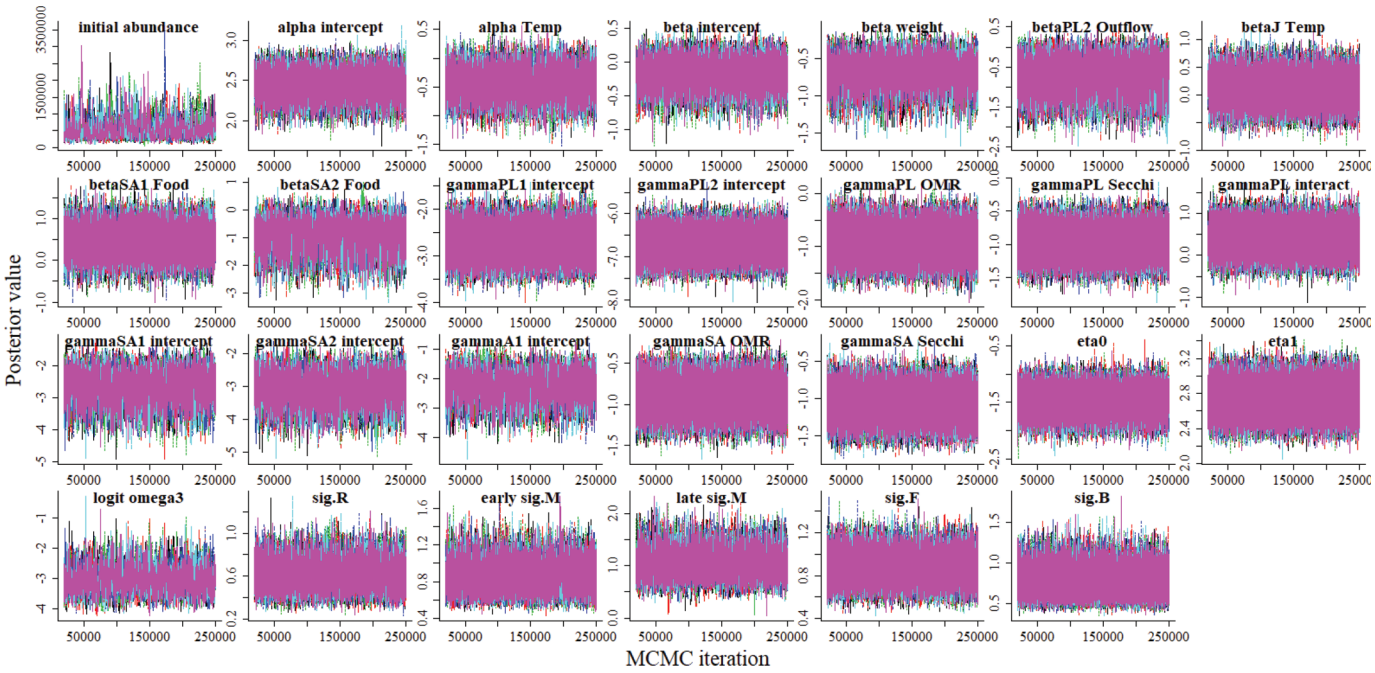

Fig. A7. Posterior (dashed lines) versus prior distributions (solid lines) of all regression coefficients for recruitment success (alpha), other mortality (*M*) intercept model, other mortality slopes (beta), entrainment mortality (gamma), and process errors (sig).

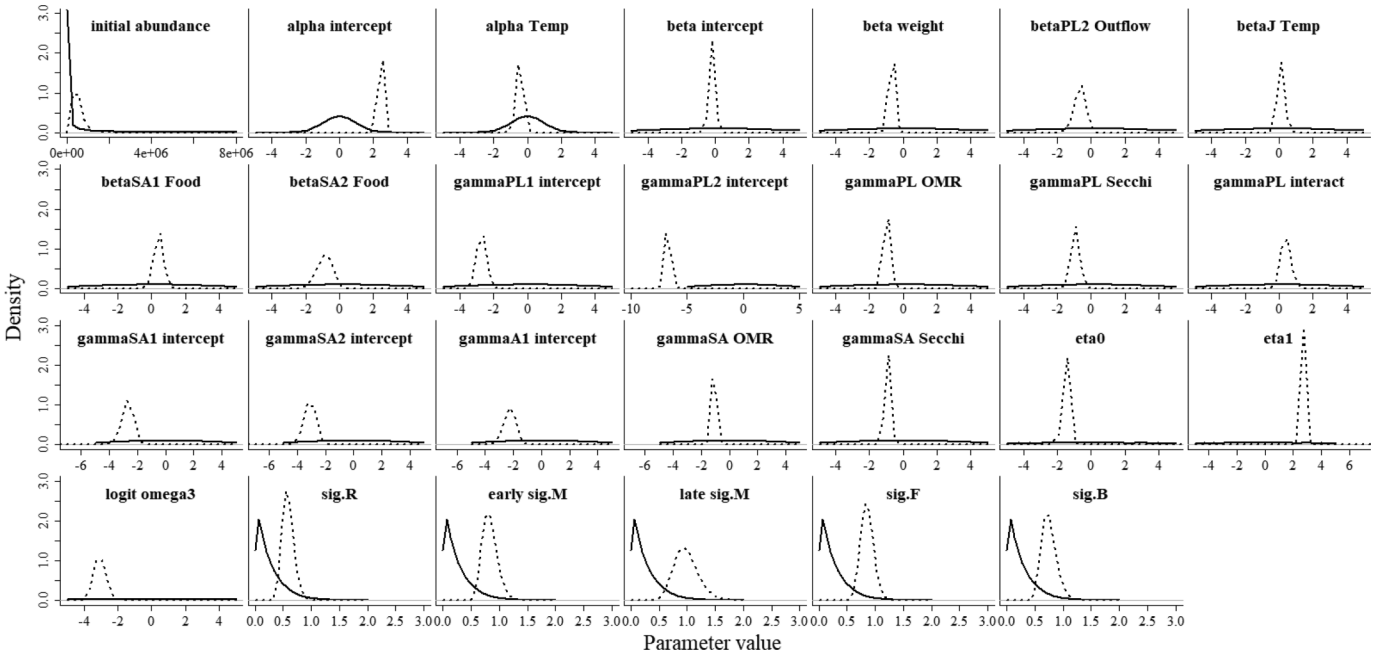

and A4). Posteriors for reproduction parameters α_0 and α_1, natural mortality regression parameters β_0–β_4, and reproduction and entrainment process variances σ_R and σ_F were highly informed by observations. Some posteriors for starting abundance and natural mortality process variance σ_M had low shrinkage values, indicating greater similarity between prior and posterior parameter distributions. These parameters may become dominated by their priors under some conditions; therefore, we checked prior versus posterior plots carefully in the life cycle model fit to delta smelt to identify this problem if it manifested.

References

Betancourt, M. 2018. Calibrating model-based inferences and decisions. arXiv:1803.08393 [stat.ME].

Plummer, M. 2003. JAGS: a program for analysis of Bayesian graphical models using Gibbs sampling. *In* Proceedings of the 3rd International Workshop on Distributed Statistical Computing, Vienna, Austria.

Simpson, D., Rue, H., Riebler, A., Martins, T.G., and Sørbye, S.H. 2017. Penalising model component complexity: a principled, practical approach to constructing priors. Stat. Sci. **32**(1): 1–28. doi:10.1214/16-STS576.

Su, Y.S., and Yajima, M. 2015. R2jags: Using R to Run 'JAGS'. Version 0.5-7. Available from https://CRAN.R-project.org/package=R2jags.